Electronic Supplementary Information (ESI) for Lab on a Chip

Electronic Supplementary Information

Pneumatic-aided micro-molding for flexible fabrication of homogeneous and heterogeneous cell-laden microgels

Chao Ma,[a] Chang Tian,[a] Lei Zhao[a] and Jinyi Wang[a,b]*

[a] *College of Veterinary Medicine, Northwest A&F University, Yangling, Shaanxi 712100, China.*

[b] *College of Science, Northwest A&F University, Yangling, Shaanxi 712100, China.*

**Phone: + 86-29-870 825 20. Fax: + 86-29-870 825 20. E-mail: jywang@nwsuaf.edu.cn.*

Abstract. This Supplementary Information includes all additional information as noted in the text.

Supplementary Figure S1.

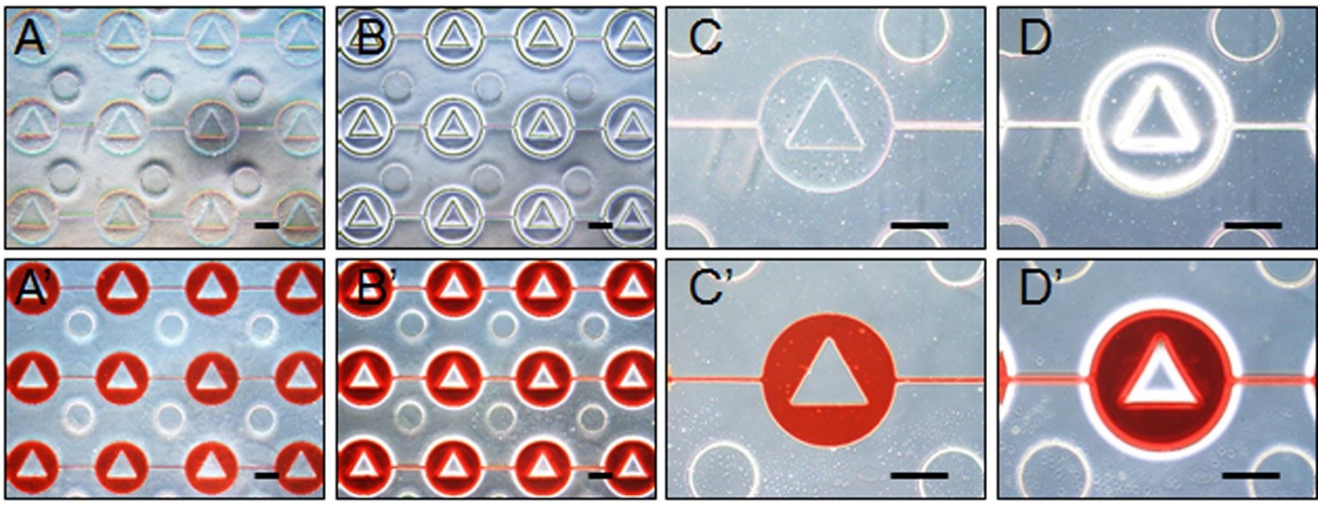

Figure S1. Display of the microfluidic device for generation of cell-laden microgel of triangular prism. (A) Bright-field image of the pneumatic microvalves in an array. (B) The actuation status of microvalves in an array. (C) Bright-field image of a single microvalve. (D) The actuation status of a single microvalve. (A')-(D') The control channel of the microvalve was colored by being filled with red food dye, corresponding to (A)-(D). Scale bar, 250 μm.

Supplementary Figure S2.

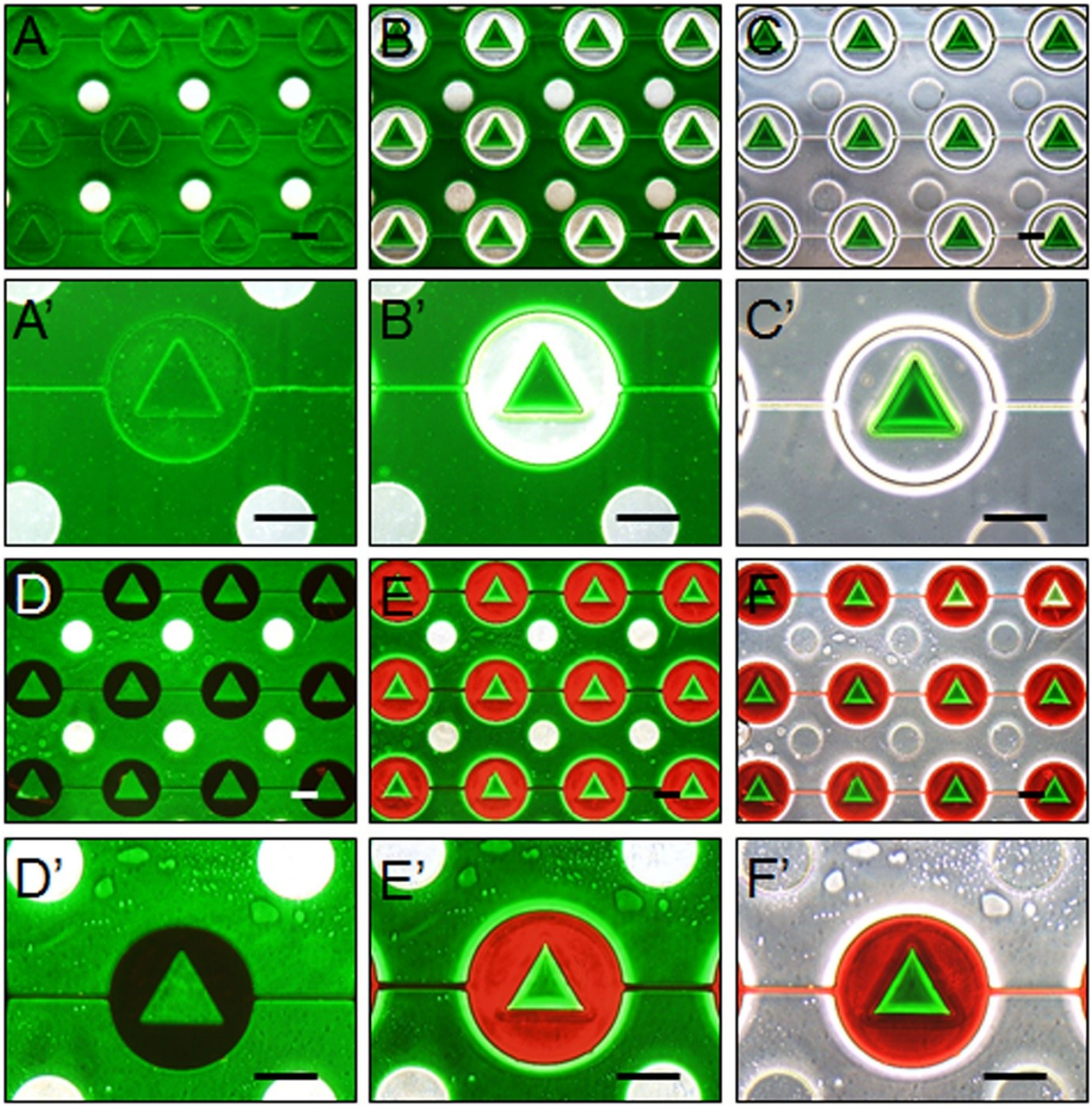

Figure S2. Display of the working flow of the microfluidic device for generation of cell-laden microgel of triangular prism. (A) The microfluidic device was filled with green food dye. (B) The pneumatic microvalves were actuated to restrict food dye in a triangle pattern. (C) A wash with water removed the unblocked food dye, which presented an array-like arrangement of food dyes with triangle shape. (A')-(C') The actuation status of a single microvalve, corresponding to (A)-(C). (D)-(F) and (D')-(F') The control channel of the microvalve was colored by being filled with red food dye, corresponding to (A)-(C) and (A')-(C'). Scale bar, 250 μm.

Supplementary Figure S3.

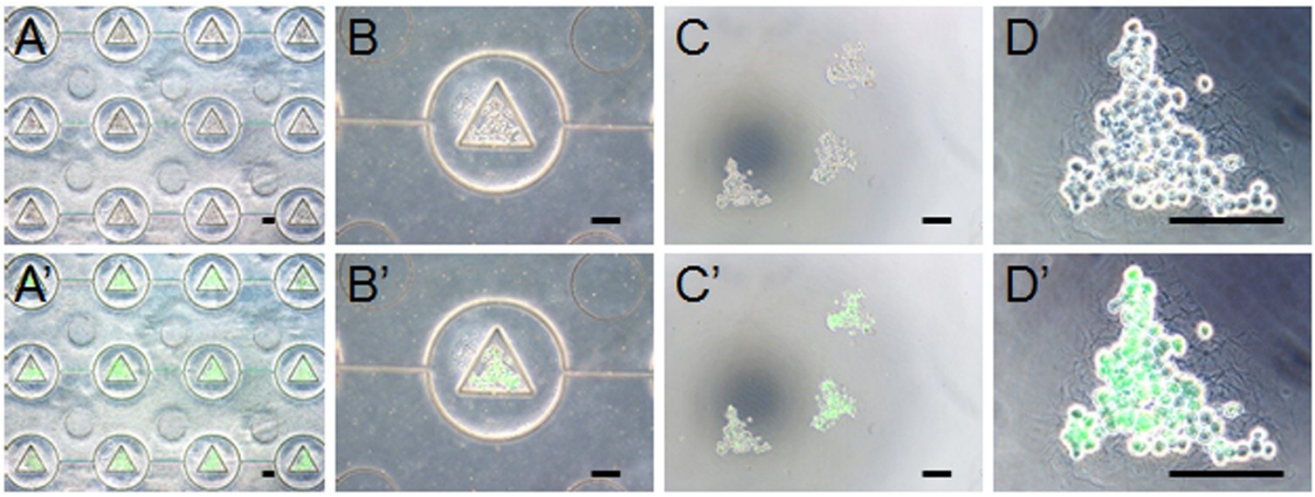

Figure S3. Generation of cell-laden microgels of triangular prism, corresponding to Figure 1B. (A) An on-chip array of cell-laden microgels. (B) A single microgel on-chip. (C) Microgels were harvested into cell culture media. (D) A single microgel harvested. (A')-(D') The merged images of bright-field images and fluorescent images, corresponding to (A)-(D). Scale bar, 125 μm.

Supplementary Figure S4.

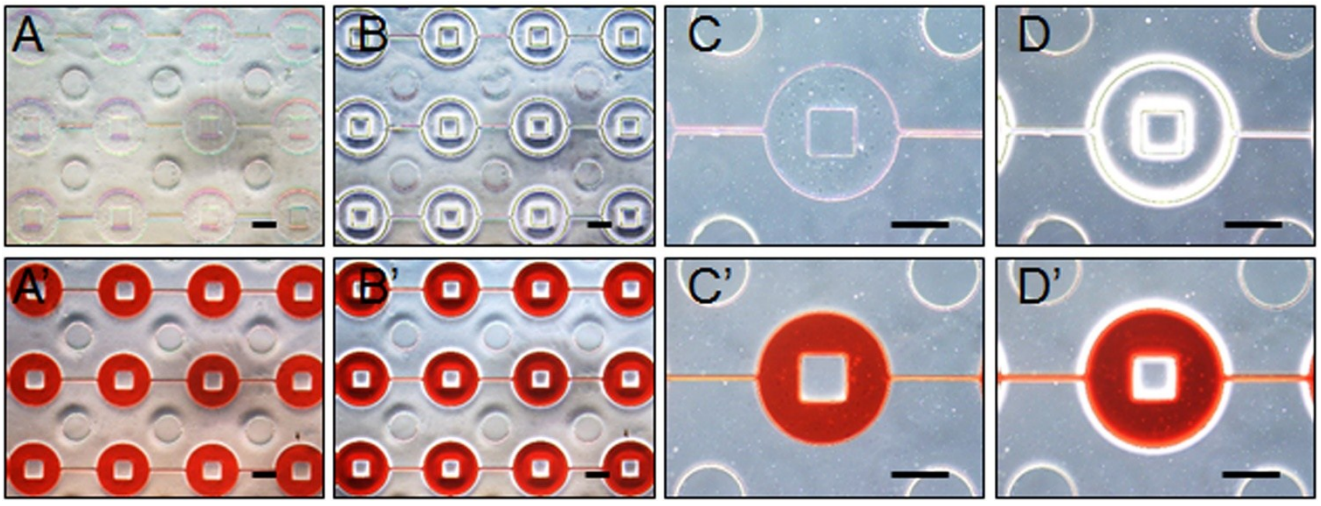

Figure S4. Display of the microfluidic device for generation of cell-laden microgel of quadrangular prism. (A) Bright-field image of the pneumatic microvalves in an array. (B) The actuation status of microvalves in an array. (C) Bright-field image of a single microvalve. (D) The actuation status of a single microvalve. (A')-(D') The control channel of the microvalve was colored by being filled with red food dye, corresponding to (A)-(D). Scale bar, 250 μm.

Supplementary Figure S5.

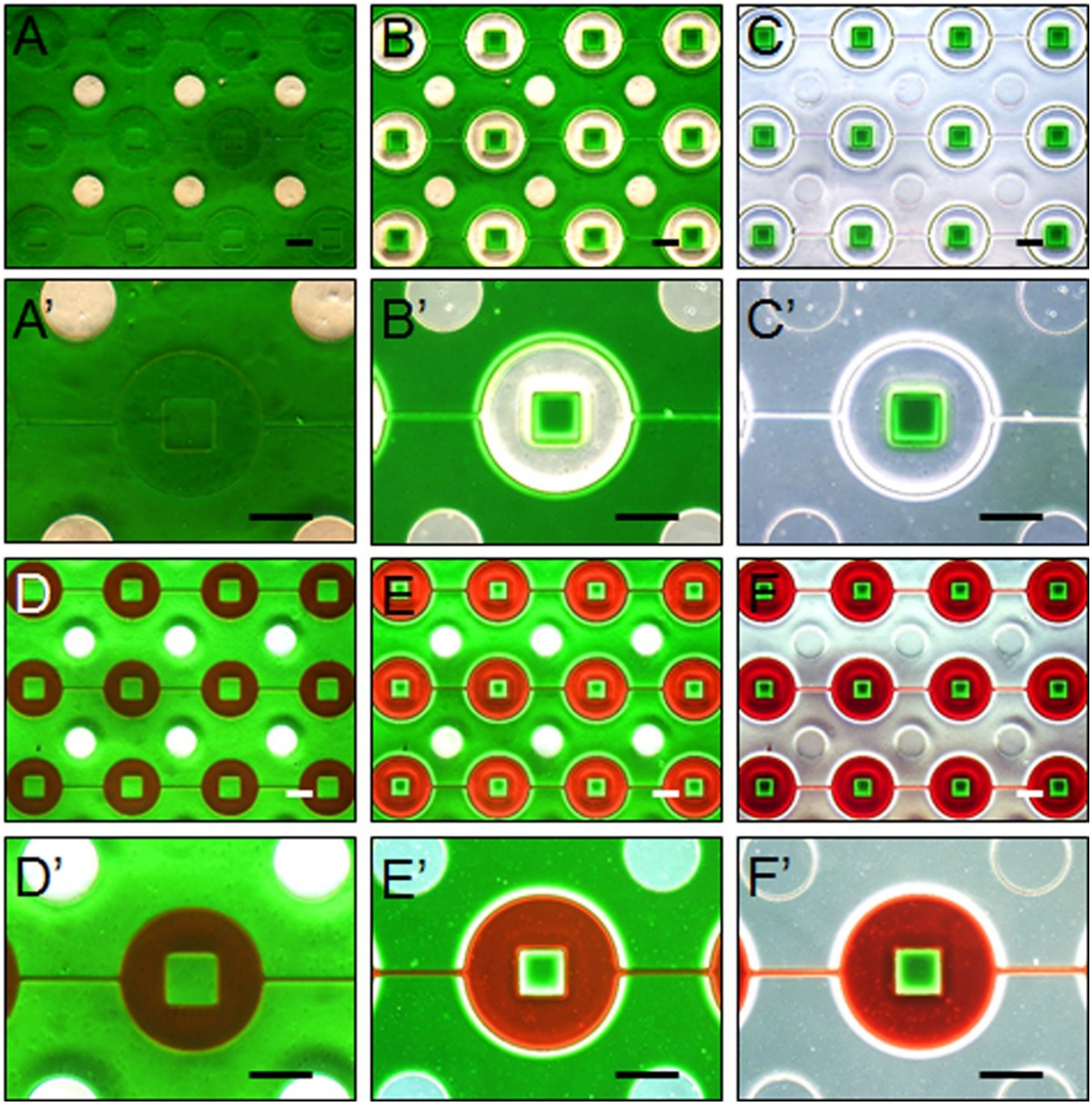

Figure S5. Display of the working flow of the microfluidic device for generation of cell-laden microgel of quadrangular prism. (A) The microfluidic device was filled with green food dye. (B) The pneumatic microvalves were actuated to restrict food dye in a square pattern. (C) A wash with water removed the unblocked food dye, which presented an array-like arrangement of food dyes with square shape. (A')-(C') The actuation status of a single microvalve, corresponding to (A)-(C). (D)-(F) and (D')-(F') The control channel of the microvalve was colored by being filled with red food dye, corresponding to (A)-(C) and (A')-(C'). Scale bar, 250 μm.

Supplementary Figure S6.

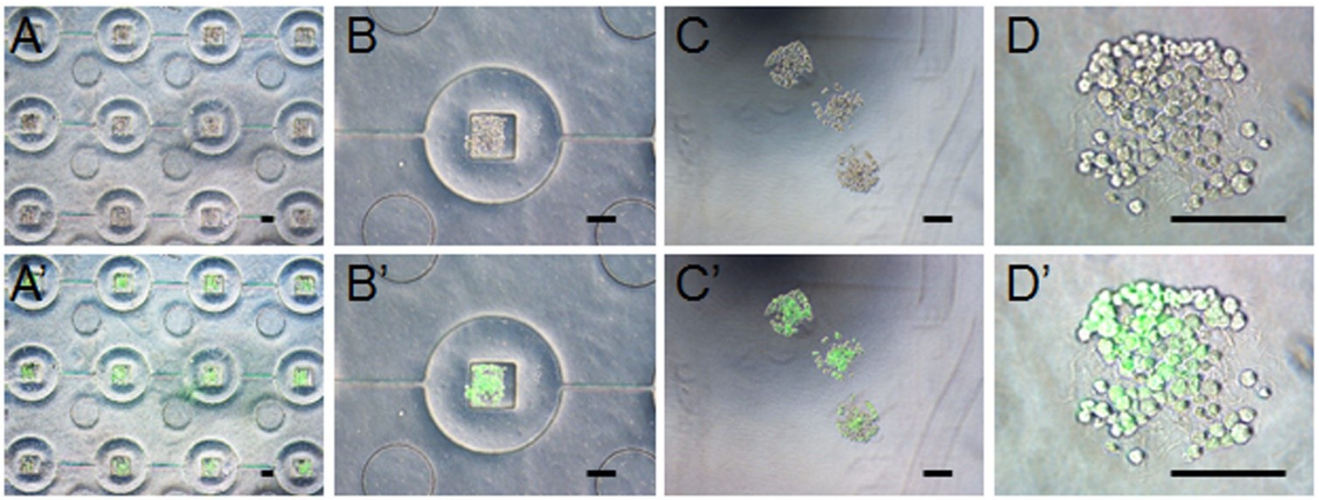

Figure S6. Generation of cell-laden microgels of quadrangular prism, corresponding to Figure 1C. (A) An on-chip array of cell-laden microgels. (B) A single microgel on-chip. (C) Microgels were harvested into cell culture media. (D) A single microgel harvested. (A')-(D') The merged images of bright-field images and fluorescent images, corresponding to (A)-(D). Scale bar, 125 μm.

Supplementary Figure S7.

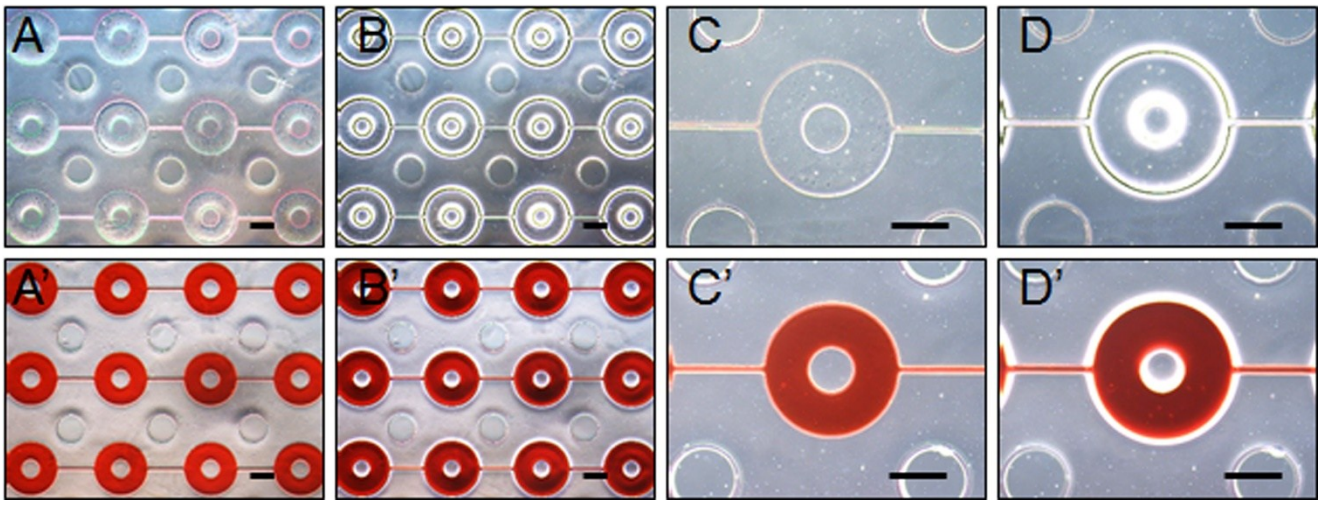

Figure S7. Display of the microfluidic device for generation of cell-laden microgel of cylinder. (A) Bright-field image of the pneumatic microvalves in an array. (B) The actuation status of microvalves in an array. (C) Bright-field image of a single microvalve. (D) The actuation status of a single microvalve. (A')-(D') The control channel of the microvalve was colored by being filled with red food dye, corresponding to (A)-(D). Scale bar, 250 μm.

Supplementary Figure S8.

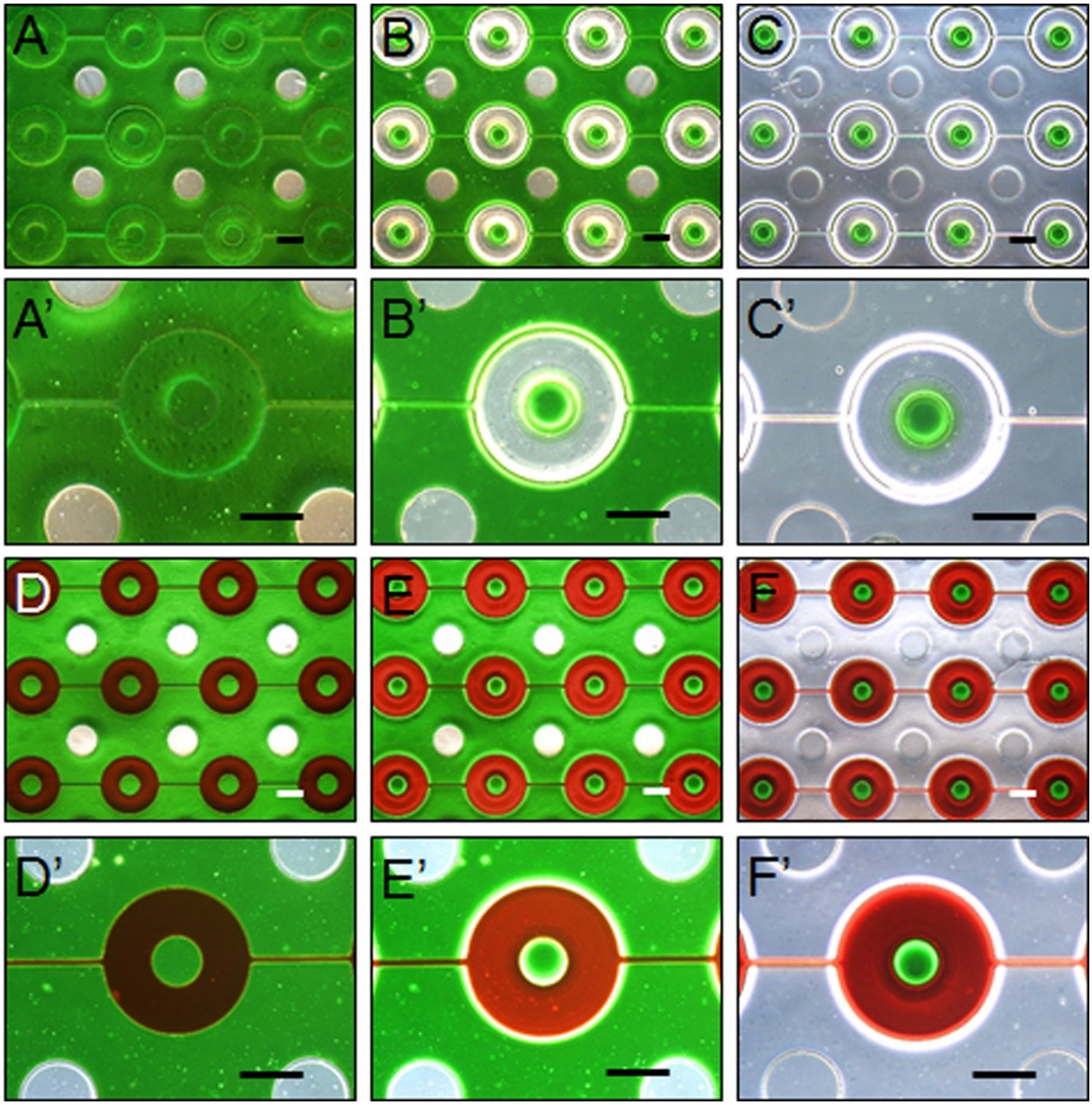

Figure S8. Display of the working flow of the microfluidic device for generation of cell-laden microgel of cylinder. (A) The microfluidic device was filled with green food dye. (B) The pneumatic microvalves were actuated to restrict food dye in a circular pattern. (C) A wash with water removed the unblocked food dye, which presented an array-like arrangement of food dyes with circle shape. (A')-(C') The actuation status of a single microvalve, corresponding to (A)-(C). (D)-(F) and (D')-(F') The control channel of the microvalve was colored by being filled with red food dye, corresponding to (A)-(C) and (A')-(C'). Scale bar, 250 μm.

Supplementary Figure S9.

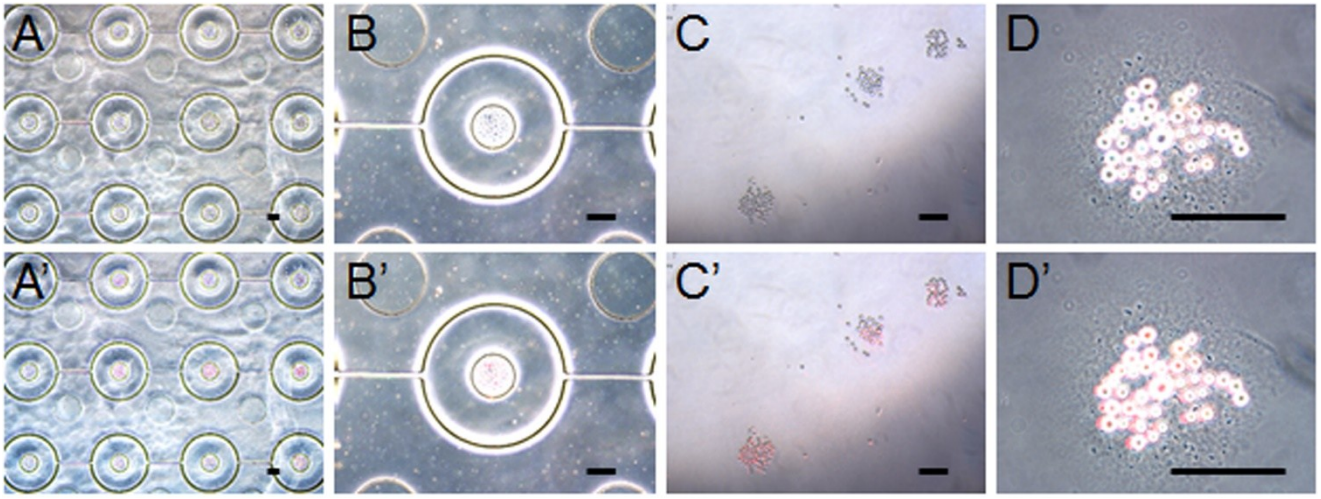

Figure S9. Generation of cell-laden microgels of cylinder, corresponding to Figure 1D. (A) An on-chip array of cell-laden microgels. (B) A single microgel on-chip. (C) Microgels were harvested into cell culture media. (D) A single microgel harvested. (A')-(D') The merged images of bright-field images and fluorescent images, corresponding to (A)-(D). Scale bar, 125 μm.

Supplementary Figure S10.

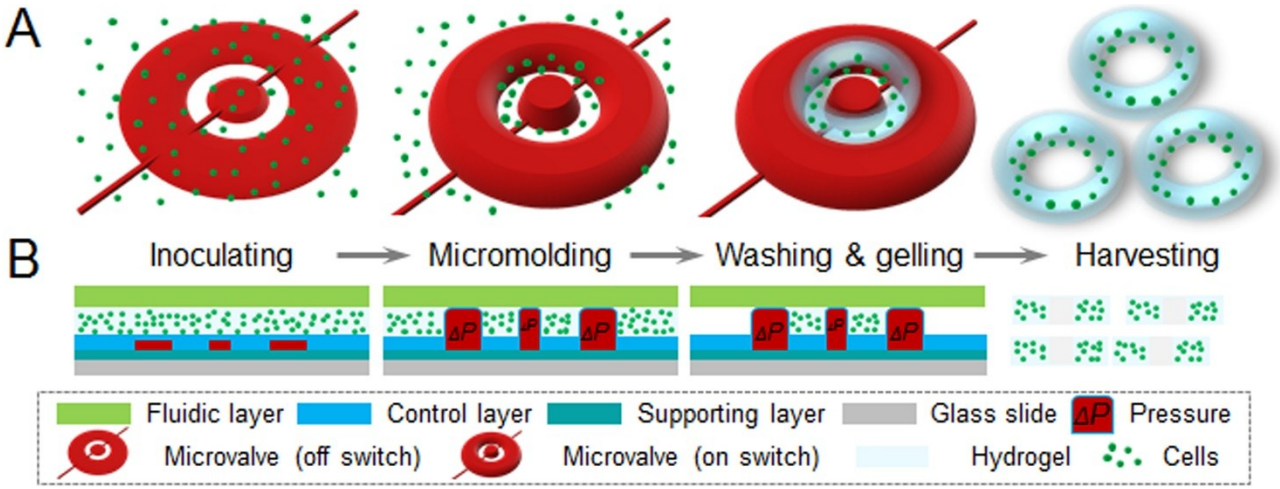

Figure S10. Schematic illustrating the fabricating process of single micro-channeled cell-laden microgels. As shown in (A), a redesigned microvalve was engineered, which comprised two parts of valve structures interconnected through bypass control channels. The width of the bypass control channel was set to 25 μm, which showed no spatial deformation under a certain gas pressure. (A) Three-dimensional view of the PAM process. (B) Cross-sectional view of the working status of microvalves during PAM.

Supplementary Figure S11.

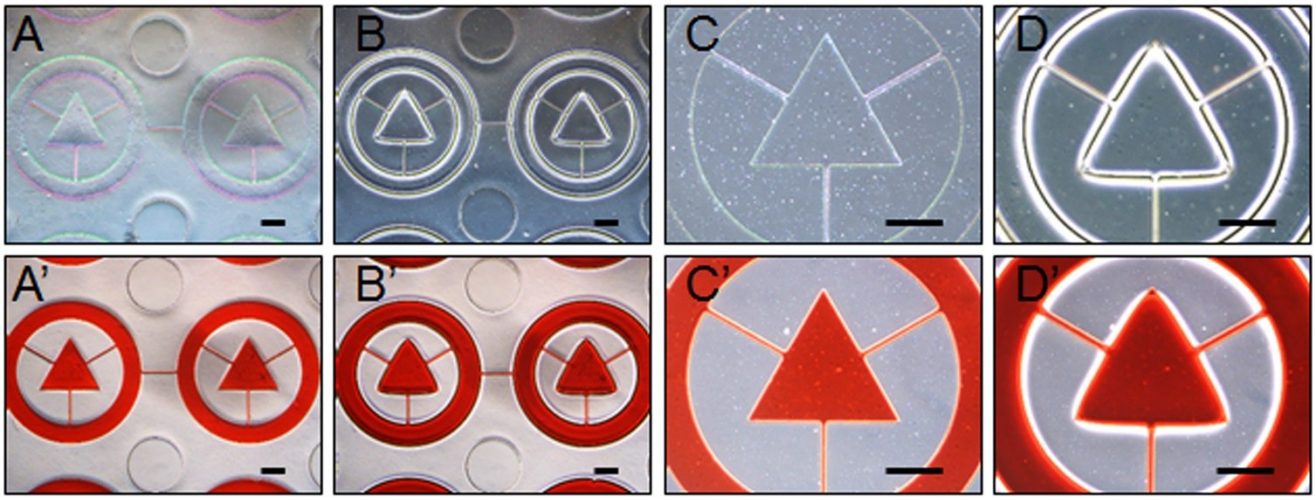

Figure S11. Display of the microfluidic device for generation of cell-laden microgel with a single triangular micro-channel. (A) Bright-field image of the pneumatic microvalves in an array. (B) The actuation status of microvalves in an array. (C) Bright-field image of a single microvalve. (D) The actuation status of a single microvalve. (A')-(D') The control channel of the microvalve was colored by being filled with red food dye, corresponding to (A)-(D). Scale bar, 250 μm.

Supplementary Figure S12.

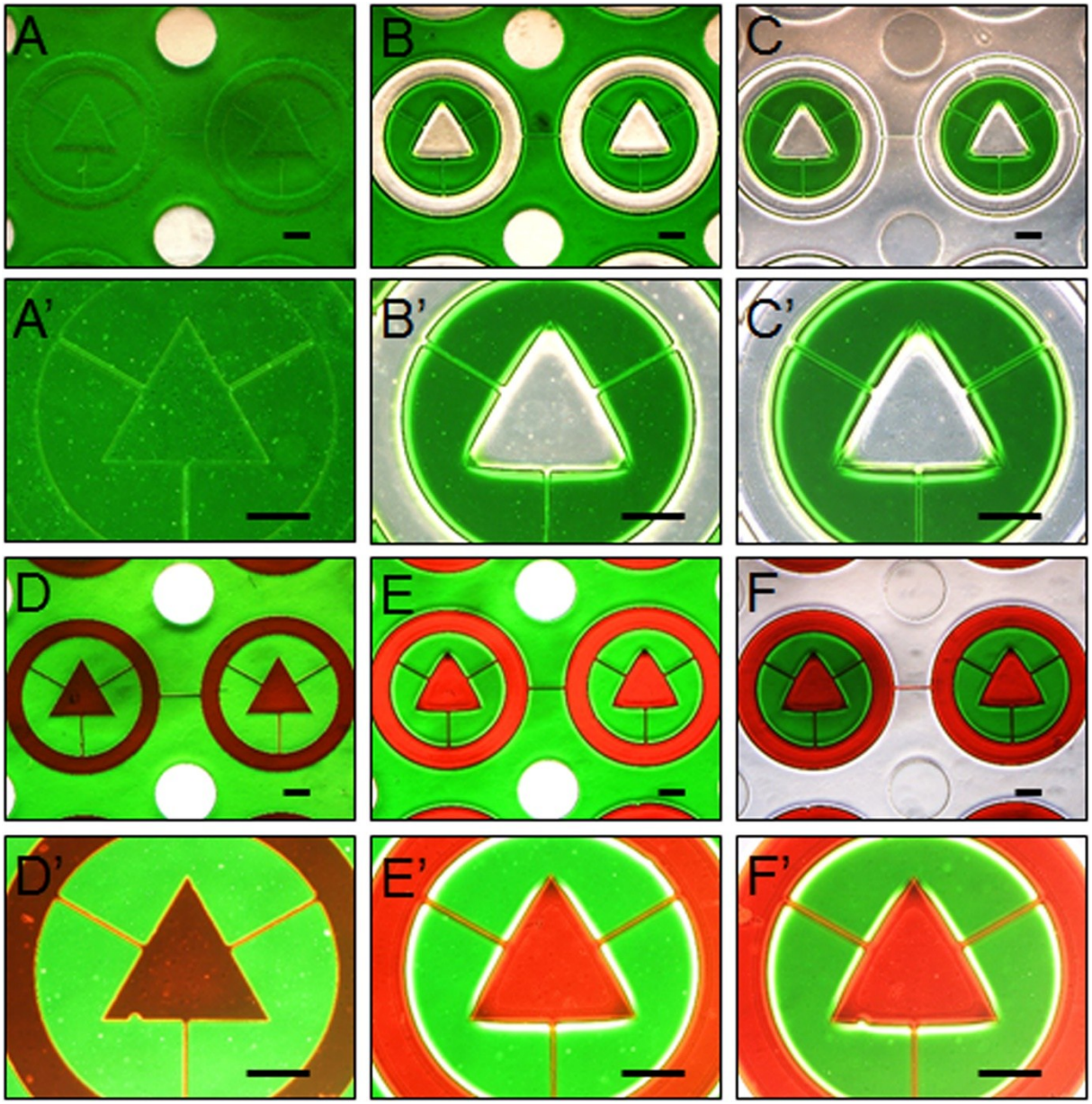

Figure S12. Display of the working flow of the microfluidic device for generation of cell-laden microgel with a single triangular micro-channel. (A) The microfluidic device was filled with green food dye. (B) The pneumatic microvalves were actuated to restrict food dye. (C) A wash with water removed the unblocked food dye. (A')-(C') The actuation status of a single microvalve, corresponding to (A)-(C). (D)-(F) and (D')-(F') The control channel of the microvalve was colored by being filled with red food dye, corresponding to (A)-(C) and (A')-(C'). Scale bar, 250 μm.

Supplementary Figure S13.

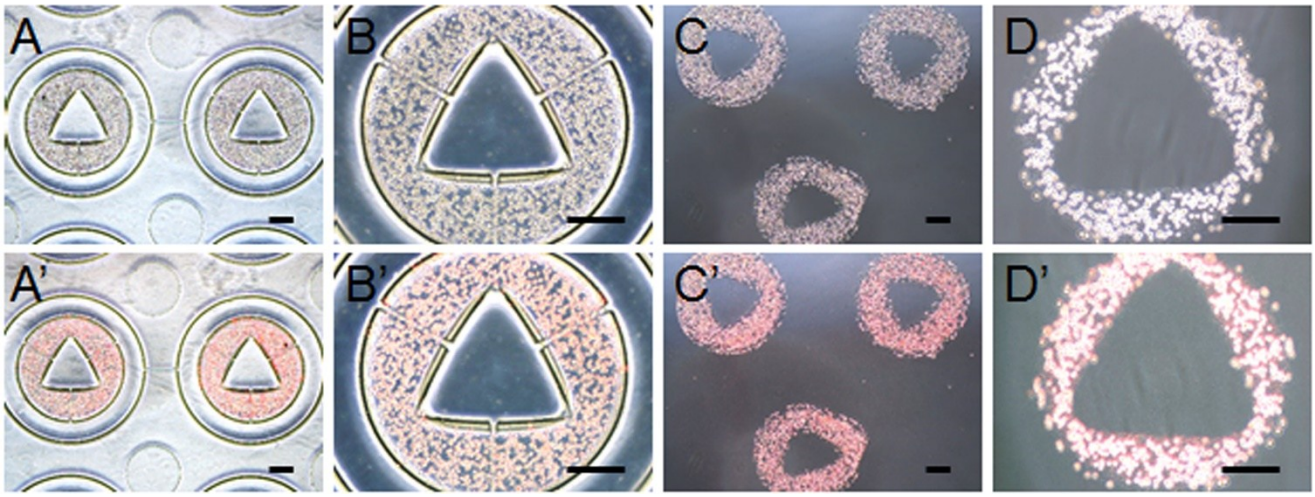

Figure S13. Generation of cell-laden microgels with a single triangular micro-channel, corresponding to Figure 2A (**Play-button**). (A) An on-chip array of cell-laden microgels. (B) A single microgel on-chip. (C) Microgels were harvested into cell culture media. (D) A single microgel harvested. (A')-(D') The merged images of bright-field and fluorescent images, corresponding to (A)-(D). Scale bar, 250 μm.

Supplementary Figure S14.

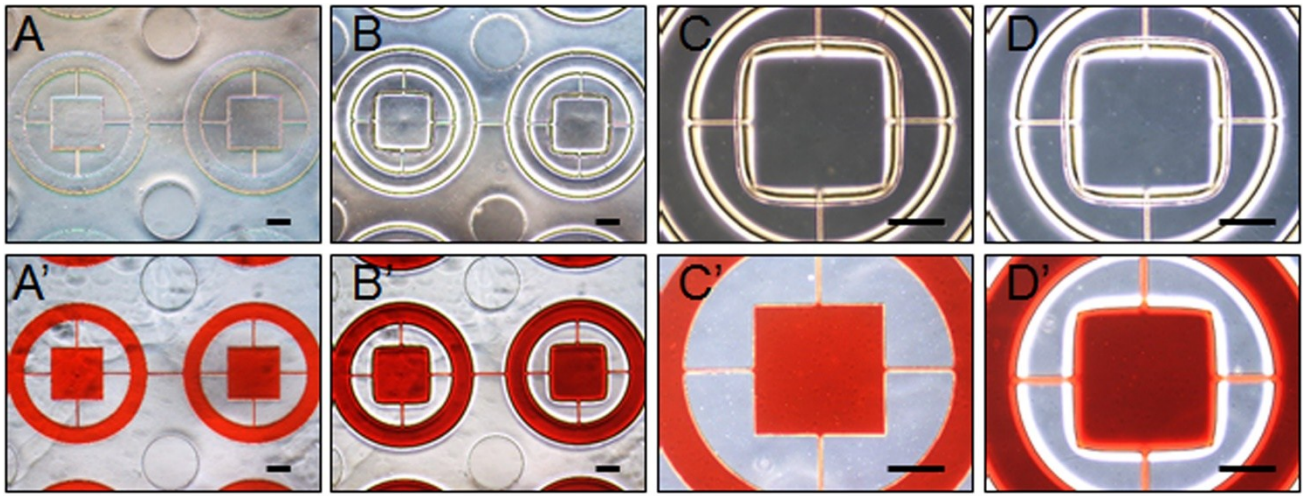

Figure S14. Display of the microfluidic device for generation of cell-laden microgel with a single square micro-channel. (A) Bright-field image of the pneumatic microvalves in an array. (B) The actuation status of microvalves in an array. (C) Bright-field image of a single microvalve. (D) The actuation status of a single microvalve. (A')-(D') The control channel of the microvalve was colored by being filled with red food dye, corresponding to (A)-(D). Scale bar, 250 μm.

Supplementary Figure S15.

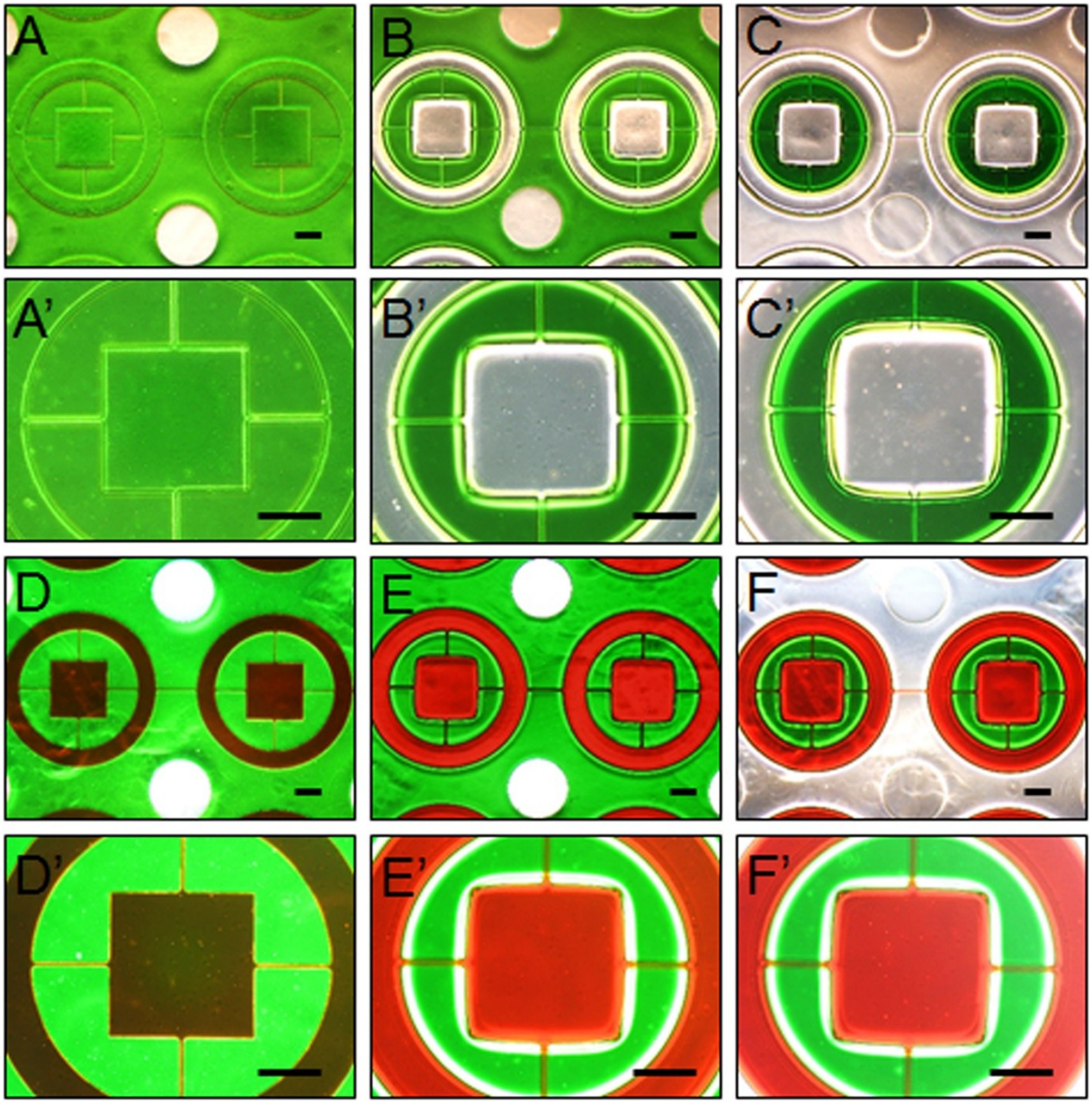

Figure S15. Display of the working flow of the microfluidic device for generation of cell-laden microgel with a single square micro-channel. (A) The microfluidic device was filled with green food dye. (B) The pneumatic microvalves were actuated to restrict food dye. (C) A wash with water removed the unblocked food dye. (A')-(C') The actuation status of a single microvalve, corresponding to (A)-(C). (D)-(F) and (D')-(F') The control channel of the microvalve was colored by being filled with red food dye, corresponding to (A)-(C) and (A')-(C'). Scale bar, 250 μm.

Supplementary Figure S16.

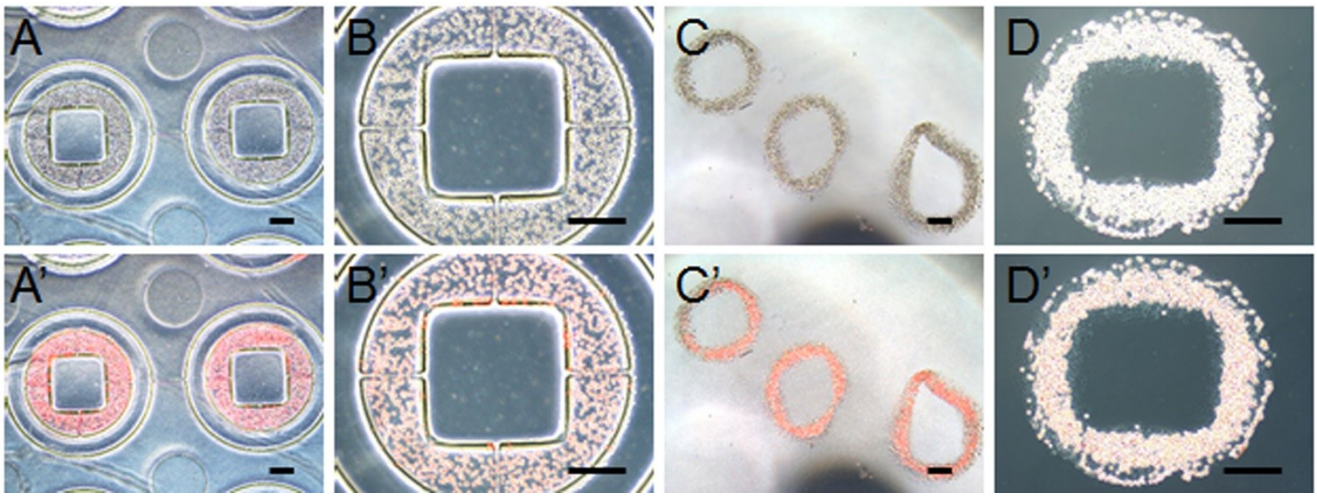

Figure S16. Generation of cell-laden microgels with a single square micro-channel, corresponding to Figure 2A (**Sapèque**). (A) An on-chip array of cell-laden microgels. (B) A single microgel on-chip. (C) Microgels were harvested into cell culture media. (D) A single microgel harvested. (A')-(D') The merged images of bright-field images and fluorescent images, corresponding to (A)-(D). Scale bar, 250 μm.

Supplementary Figure S17.

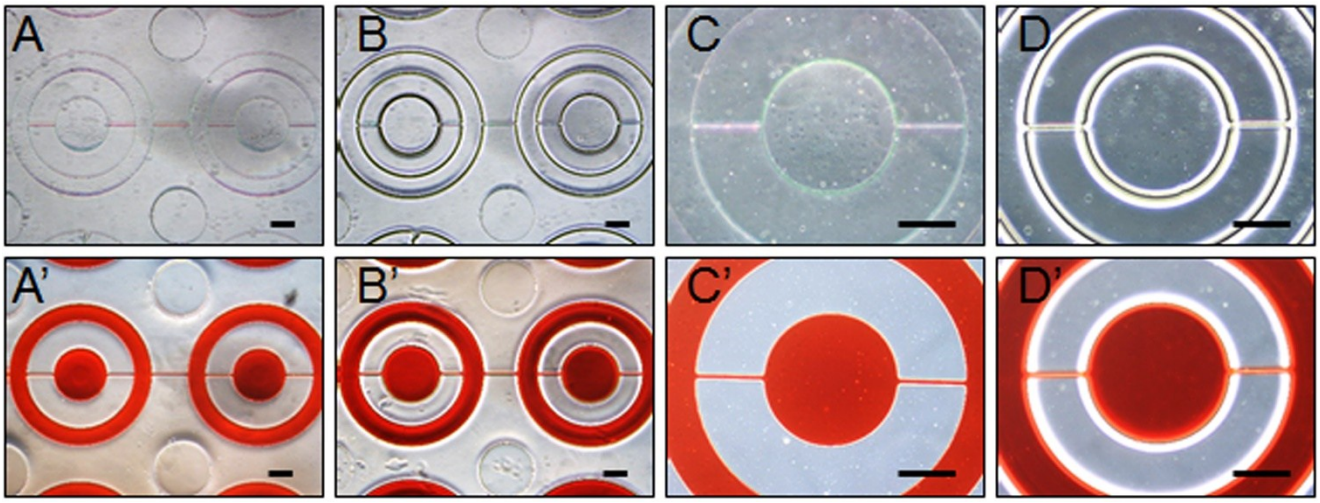

Figure S17. Display of the microfluidic device for generation of cell-laden microgel with a single circular micro-channel. (A) Bright-field image of the pneumatic microvalves in an array. (B) The actuation status of microvalves in an array. (C) Bright-field image of a single microvalve. (D) The actuation status of a single microvalve. (A')-(D') The control channel of the microvalve was colored by being filled with red food dye, corresponding to (A)-(D). Scale bar, 250 μm.

Supplementary Figure S18.

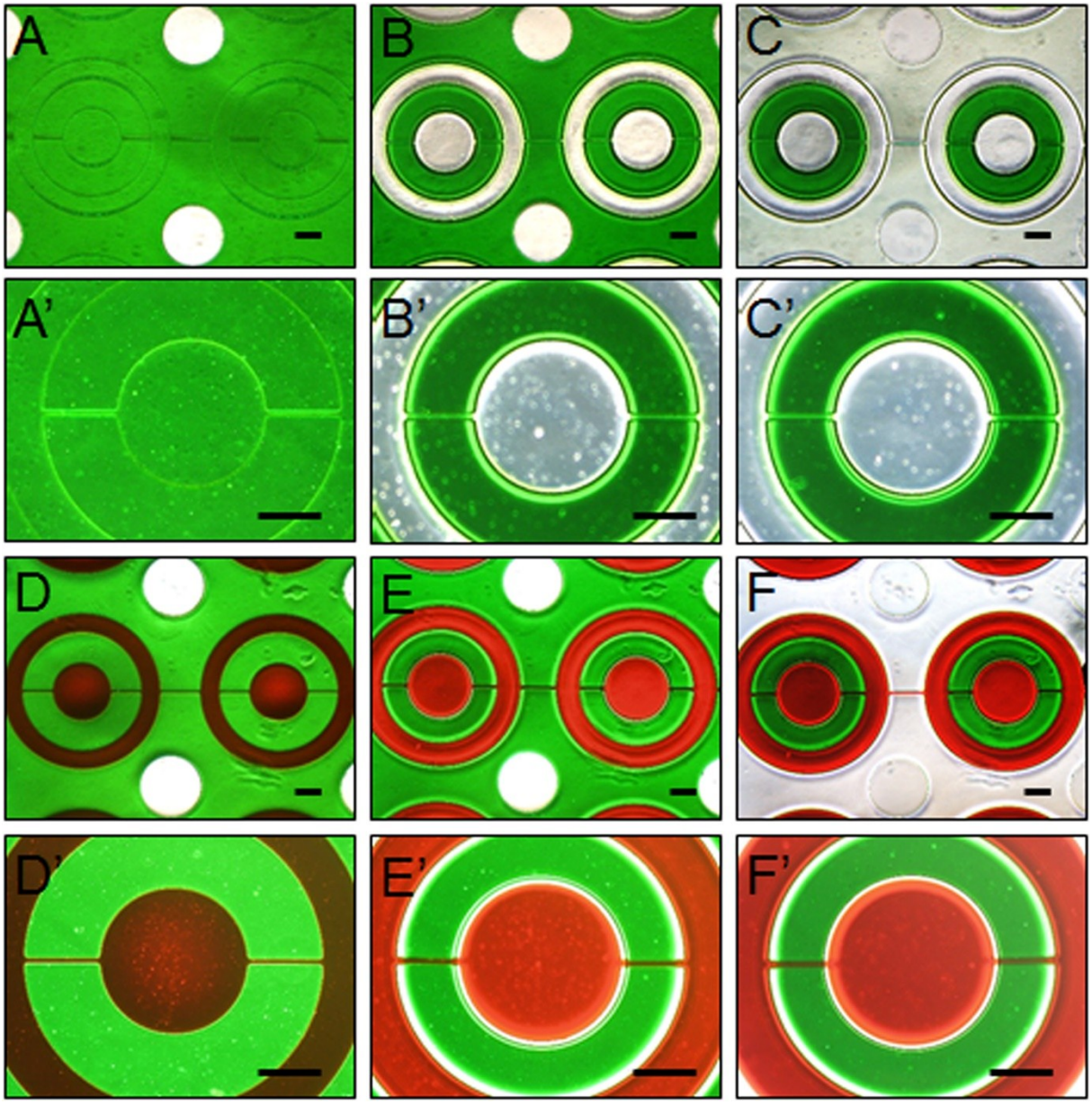

Figure S18. Display of the working flow of the microfluidic device for generation of cell-laden microgel with a single circular micro-channel. (A) The microfluidic device was filled with green food dye. (B) The pneumatic microvalves were actuated to restrict food dye. (C) A wash with water removed the unblocked food dye. (A')-(C') The actuation status of a single microvalve, corresponding to (A)-(C). (D)-(F) and (D')-(F') The control channel of the microvalve was colored by being filled with red food dye, corresponding to (A)-(C) and (A')-(C'). Scale bar, 250 μm.

Supplementary Figure S19.

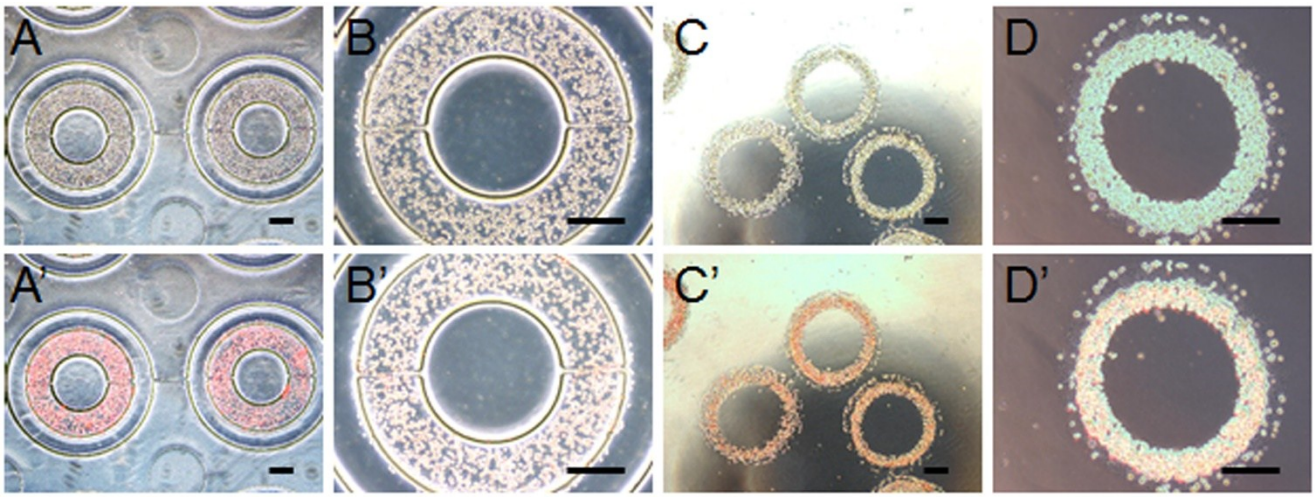

Figure S19. Generation of cell-laden microgels with a single circular micro-channel, corresponding to Figure 2A (**Donut**). (A) An on-chip array of cell-laden microgels. (B) A single microgel on-chip. (C) Microgels were harvested into cell culture media. (D) A single microgel harvested. (A')-(D') The merged images of bright-field images and fluorescent images, corresponding to (A)-(D). Scale bar, 250 μm.

Supplementary Figure S20.

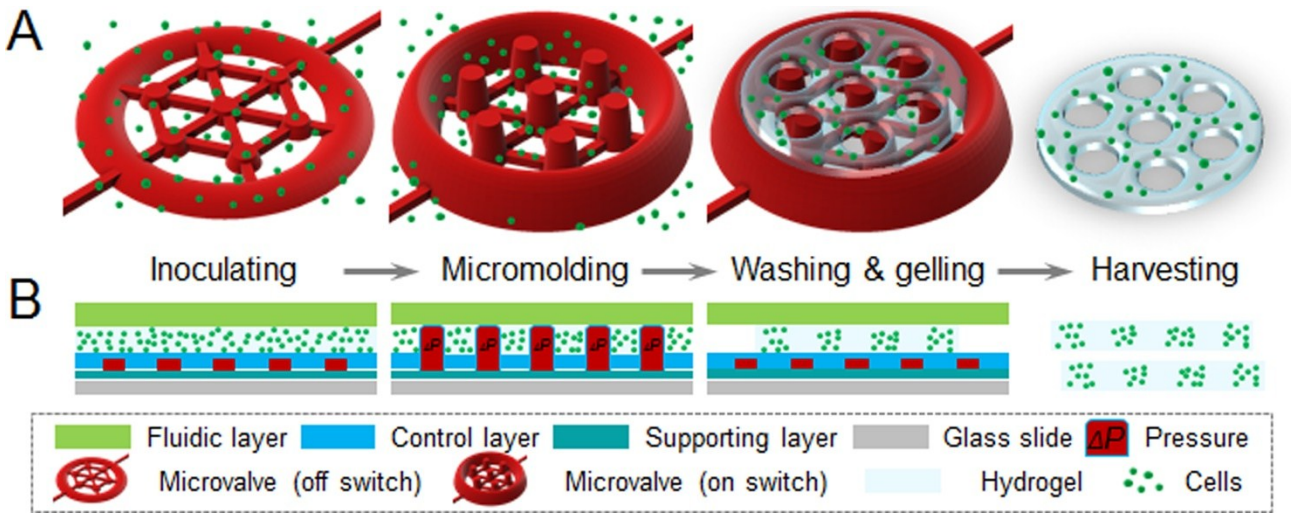

Figure S20. Schematic illustrating the fabricating process of multiple micro-channeled cell-laden microgels. (A) Three-dimensional view of the PAM process. (B) Cross-sectional view of the working status of microvalves during PAM.

Supplementary Figure S21.

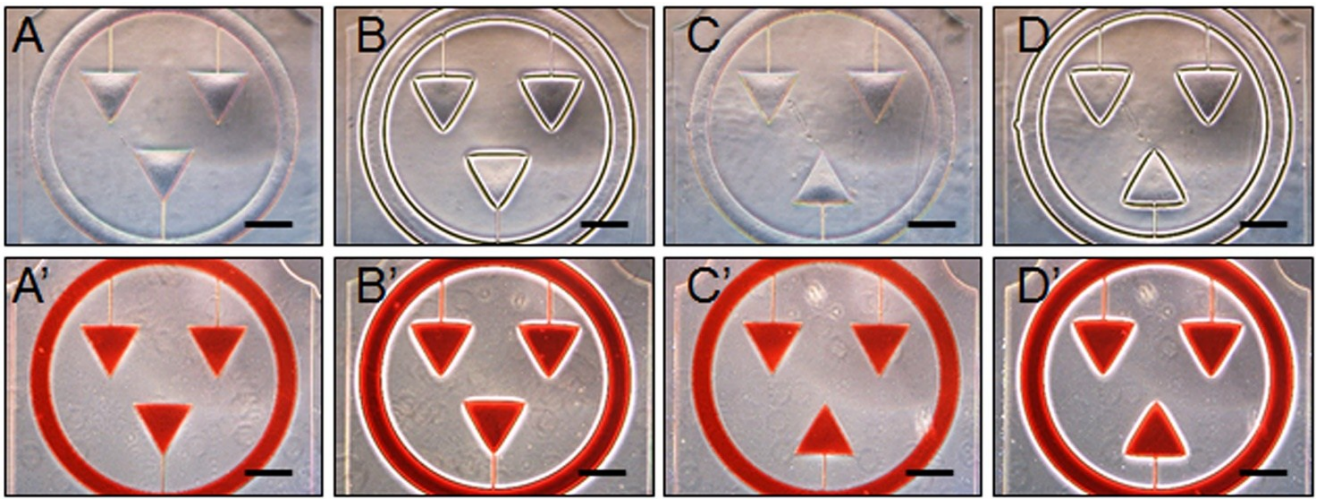

Figure S21. Display of the microfluidic device for generation of cell-laden microgel with three triangular micro-channels. (A) Bright-field image of the pneumatic microvalves in a 'smiling' face-like arrangement. (B) The actuation status of microvalves corresponding to (A). (C) Bright-field image of the pneumatic microvalves in a 'crying' face-like arrangement. (D) The actuation status of microvalves corresponding to (C). (A')-(D') The control channel of the microvalve was colored by being filled with red food dye, corresponding to (A)-(D). Scale bar, 500 μm.

Supplementary Figure S22.

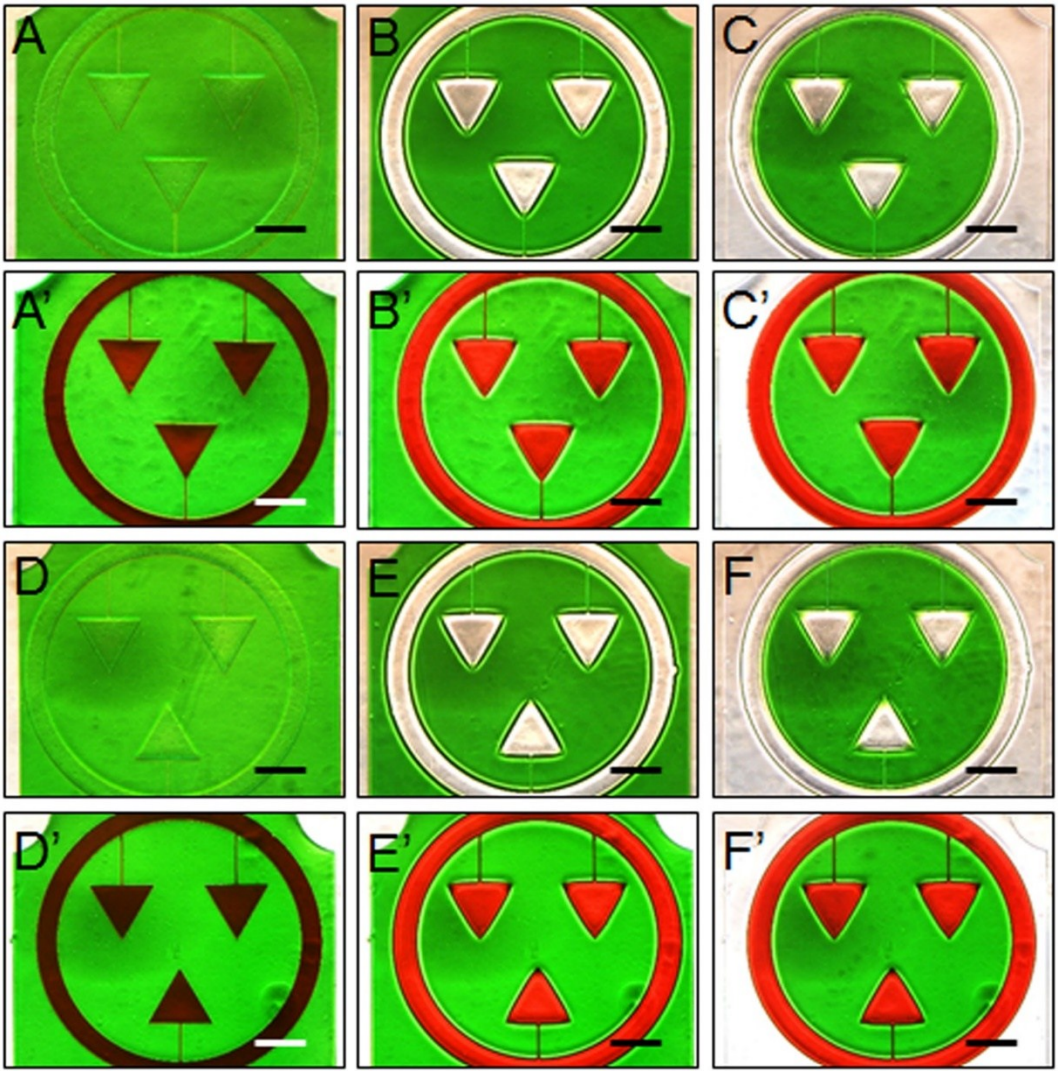

Figure S22. Display of the working flow of the microfluidic device for generation of cell-laden microgel with three triangular micro-channels in a 'smiling'/'crying' face-like arrangement. (A) and (D) The microfluidic device was filled with green food dye. (B) and (E) The pneumatic microvalves were actuated to restrict food dye. (C) and (F) A wash with water removed the unblocked food dye. (A')-(F') The control channel of the microvalve was colored by being filled with red food dye, corresponding to (A)-(F). Scale bar, 500 μm.

Supplementary Figure S23.

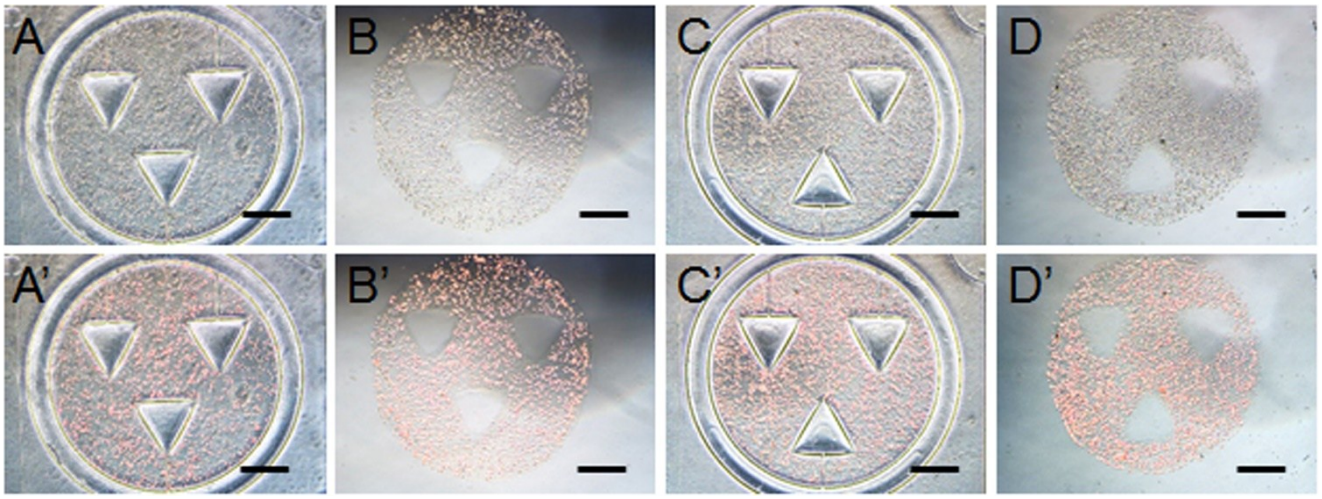

Figure S23. Generation of cell-laden microgel with three triangular micro-channels in a 'smiling'/'crying' face-like arrangement, corresponding to Figure 2B (**Smiling face** and **Crying face**). (A) A 'smiling' face-like microgel on-chip. (B) Microgels were harvested into cell culture media. (C) A 'crying' face-like microgel on-chip. (D) Microgels were harvested into cell culture media. (A')-(D') The merged images of bright-field images and fluorescent images, corresponding to (A)-(D). Scale bar, 500 μm.

Supplementary Figure S24.

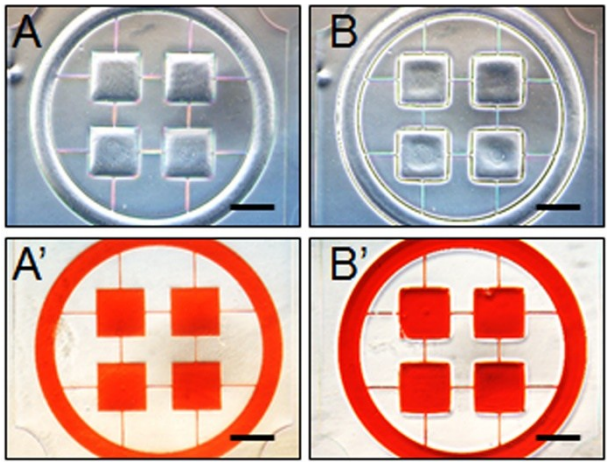

Figure S24. Display of the microfluidic device for generation of cell-laden microgel with four square micro-channels. (A) Bright-field image of the pneumatic microvalves in a windows-like arrangement. (B) The actuation status of microvalves. (A') and (B') The control channel of the microvalve was colored by

being filled with red food dye, corresponding to (A) and (B). Scale bar, 500 μm.

Supplementary Figure S25.

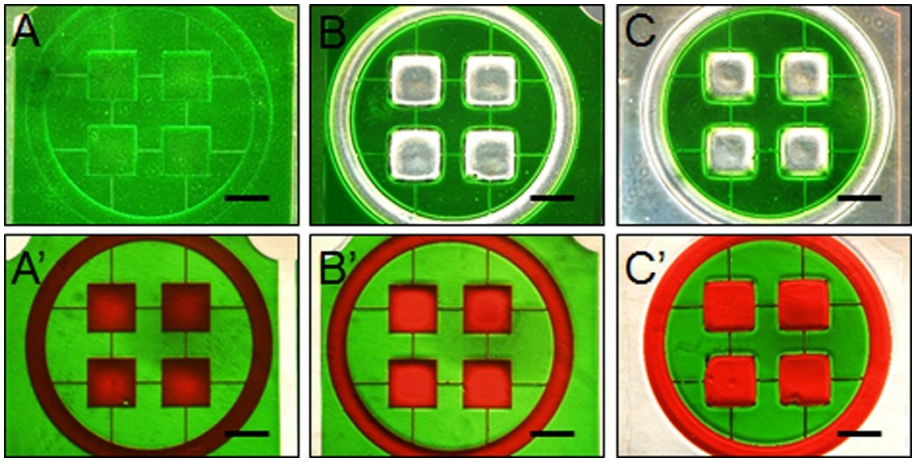

Figure S25. Display of the working flow of the microfluidic device for generation of cell-laden microgel with four square micro-channels in a windows-like arrangement. (A) The microfluidic device was filled with green food dye. (B) The pneumatic microvalves were actuated to restrict the food dye. (C) A wash with water removed the unblocked food dye. (A')-(C') The control channel of the microvalve was colored by being filled with red food dye, corresponding to (A)-(C). Scale bar, 500 μm.

Supplementary Figure S26.

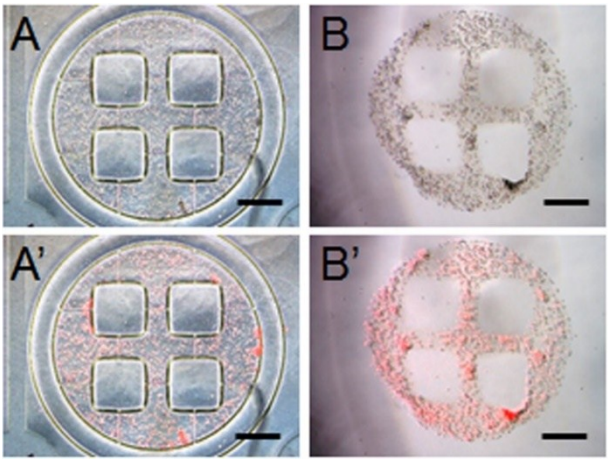

Figure S26. Generation of cell-laden microgel with four square micro-channels in a windows-like arrangement, corresponding to Figure 2B (**Windows**). (A) A windows-like microgel on-chip. (B) Microgels were harvested into cell culture media. (A') and (B') The merged images of bright-field images and fluorescent images, corresponding to (A) and (B). Scale bar, 500 μm.

Supplementary Figure S27.

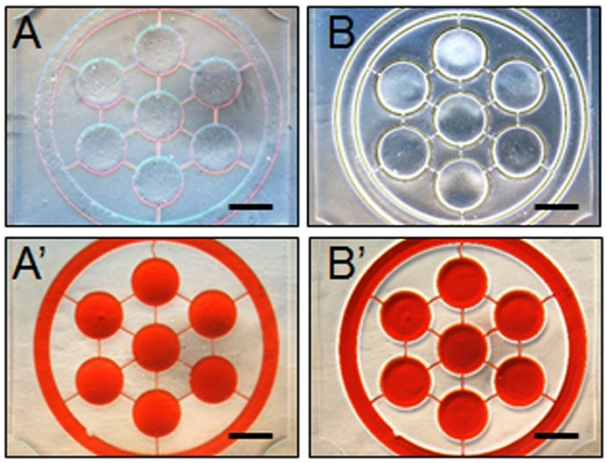

Figure S27. Display of the microfluidic device for generation of cell-laden microgel with seven circular micro-channels. (A) Bright-field image of the pneumatic microvalves in a revolver-like arrangement. (B) The actuation status of microvalves. (A') and (B') The control channel of the microvalve was colored by being filled with red food dye, corresponding to (A) and (B). Scale bar, 500 μm.

Supplementary Figure S28.

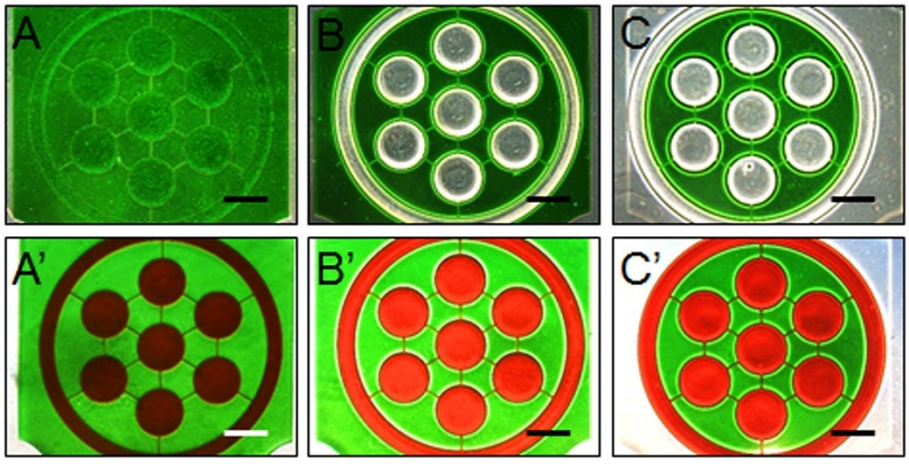

Figure S28. Display of the working flow of the microfluidic device for generation of cell-laden microgel with seven circular micro-channels in a revolver-like arrangement. (A) The microfluidic device was filled with green food dye. (B) The pneumatic microvalves were actuated to restrict the food dye. (C) A wash with water removed the unblocked food dye. (A')-(C') The control channel of the microvalve was colored by being filled with red food dye, corresponding to (A)-(C). Scale bar, 500 μm.

Supplementary Figure S29.

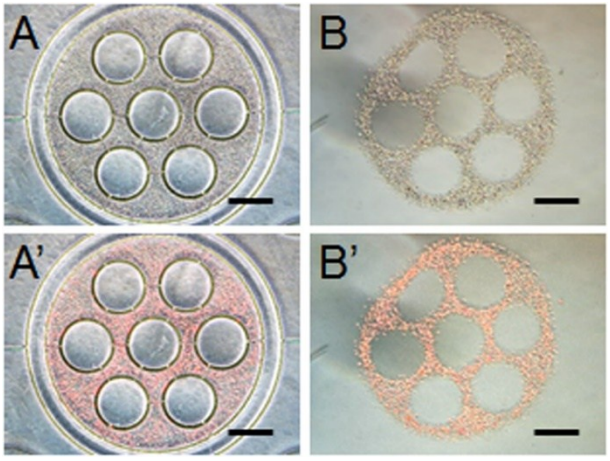

Figure S29. Generation of cell-laden microgel with seven circular micro-channels in a revolver-like arrangement, corresponding to Figure 2B (**Revolver**). (A) A revolver-like microgel on-chip. (B) Microgels were harvested into cell culture media. (A') and (B') The merged images of bright-field images and fluorescent images, corresponding to (A) and (B). Scale bar, 500 μm.

Supplementary Figure S30.

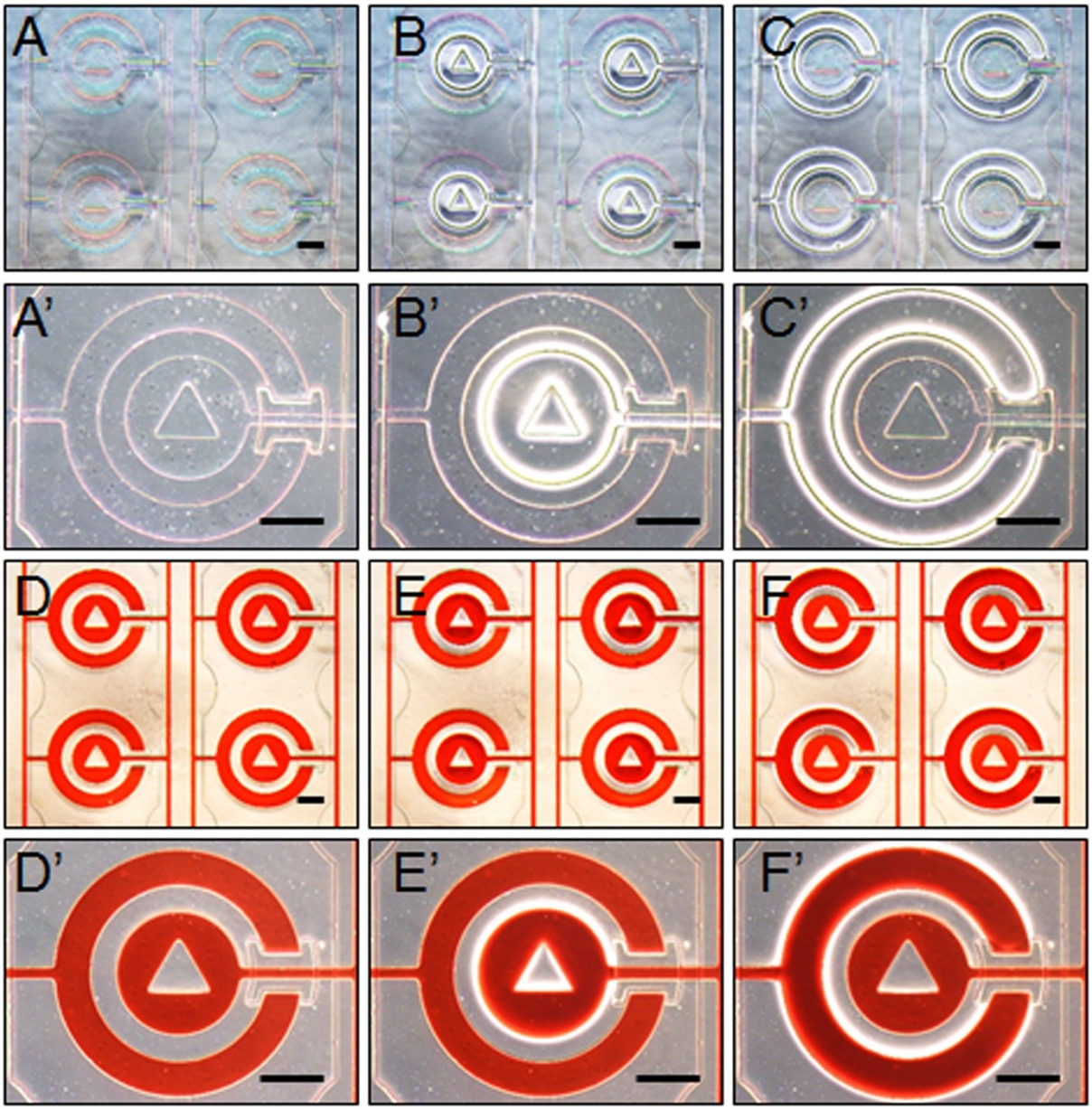

Figure S30. Display of the microfluidic device for generation of multi-compartmental cell-laden microgel with a triangular core hydrogel. (A) Bright-field image of the pneumatic microvalves in an array. (B) The actuation status of the inner ring-shape microvalves in an array. (C) The actuation status of the outer U-shape microvalves in an array. (A')-(C') The actuation status of a single microvalve, corresponding to (A)-(C). (D)-(F) and (D')-(F') The control channel of the microvalve was colored by being filled with red food dye, corresponding to (A)-(C) and (A')-(C'). Scale bar, 250 μm.

Supplementary Figure S31.

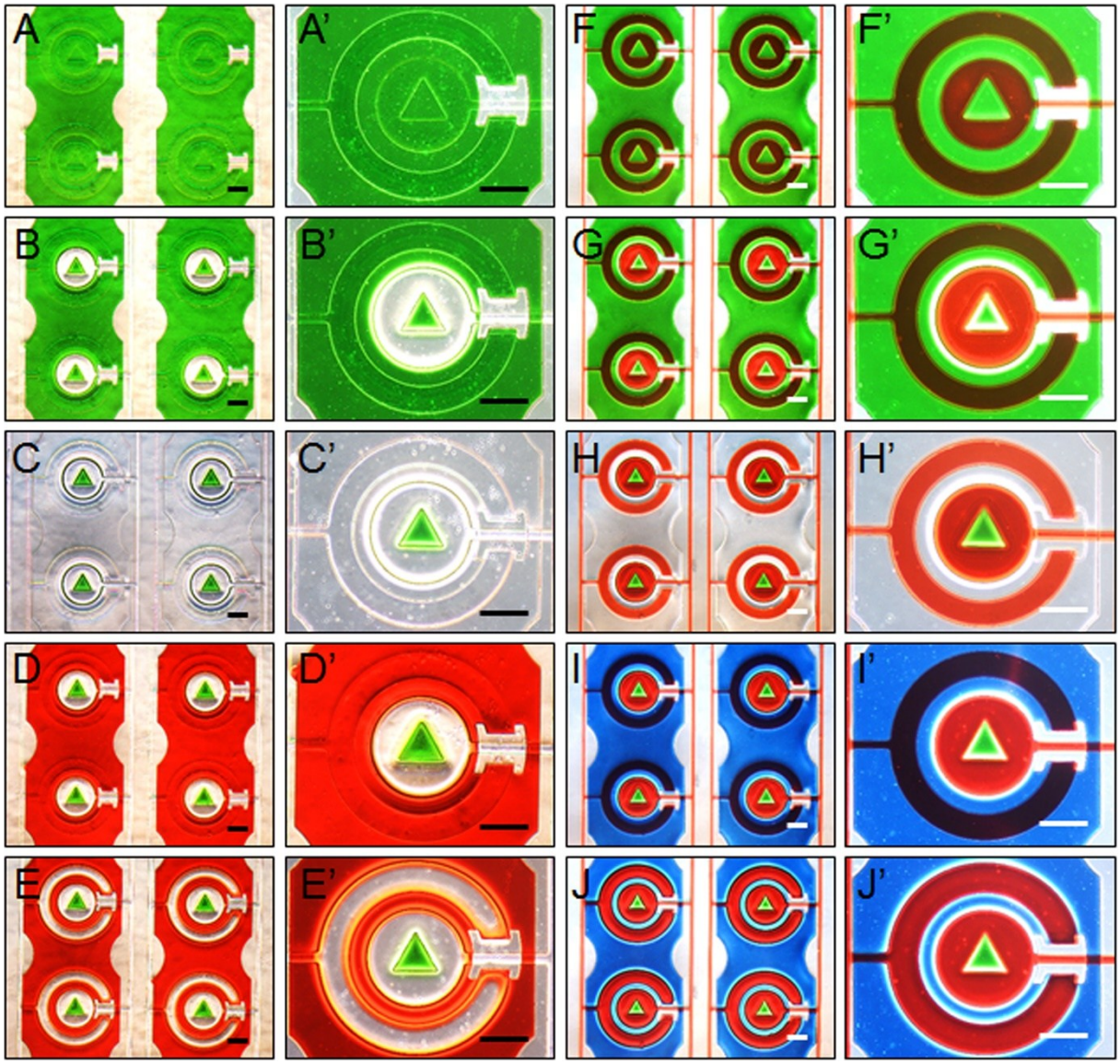

Figure S31. Display of the working flow of the microfluidic device for generation of multi-compartmental cell-laden microgel with a triangular core hydrogel. (A) The microfluidic device was filled with green food dye. (B) The inner ring-shape pneumatic microvalves were actuated to restrict the food dye in a first pattern. (C) A wash with water removed the unblocked food dye. (D) The microfluidic device was filled with red food dye. (E) The outer U-shape pneumatic microvalves were actuated to restrict the second food dye in a secondary pattern. (A')-(E') The actuation status of a single microvalve, corresponding to (A)-(E). (F)-(J) and (F')-(J') The control channel of the microvalve was colored by being filled with red food dye, corresponding to (A)-(E) and (A')-(E'). Scale bar, 250 μm.

Supplementary Figure S32.

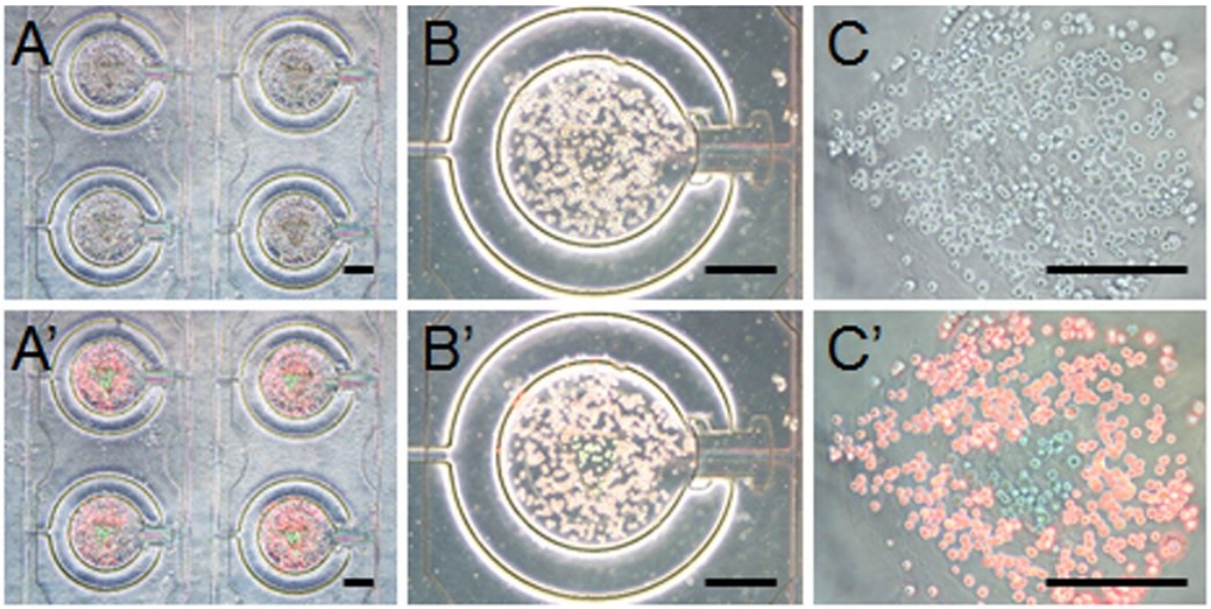

Figure S32. Generation of multi-compartmental cell-laden microgels with a triangular core hydrogel, corresponding to Figure 3B. (A) An on-chip array of cell-laden microgels. (B) A single microgel on-chip. (C) A single microgel harvested. (A')-(C') The merged images of bright-field images and fluorescent images, corresponding to (A)-(C). Scale bar, 250 μm.

Supplementary Figure S33.

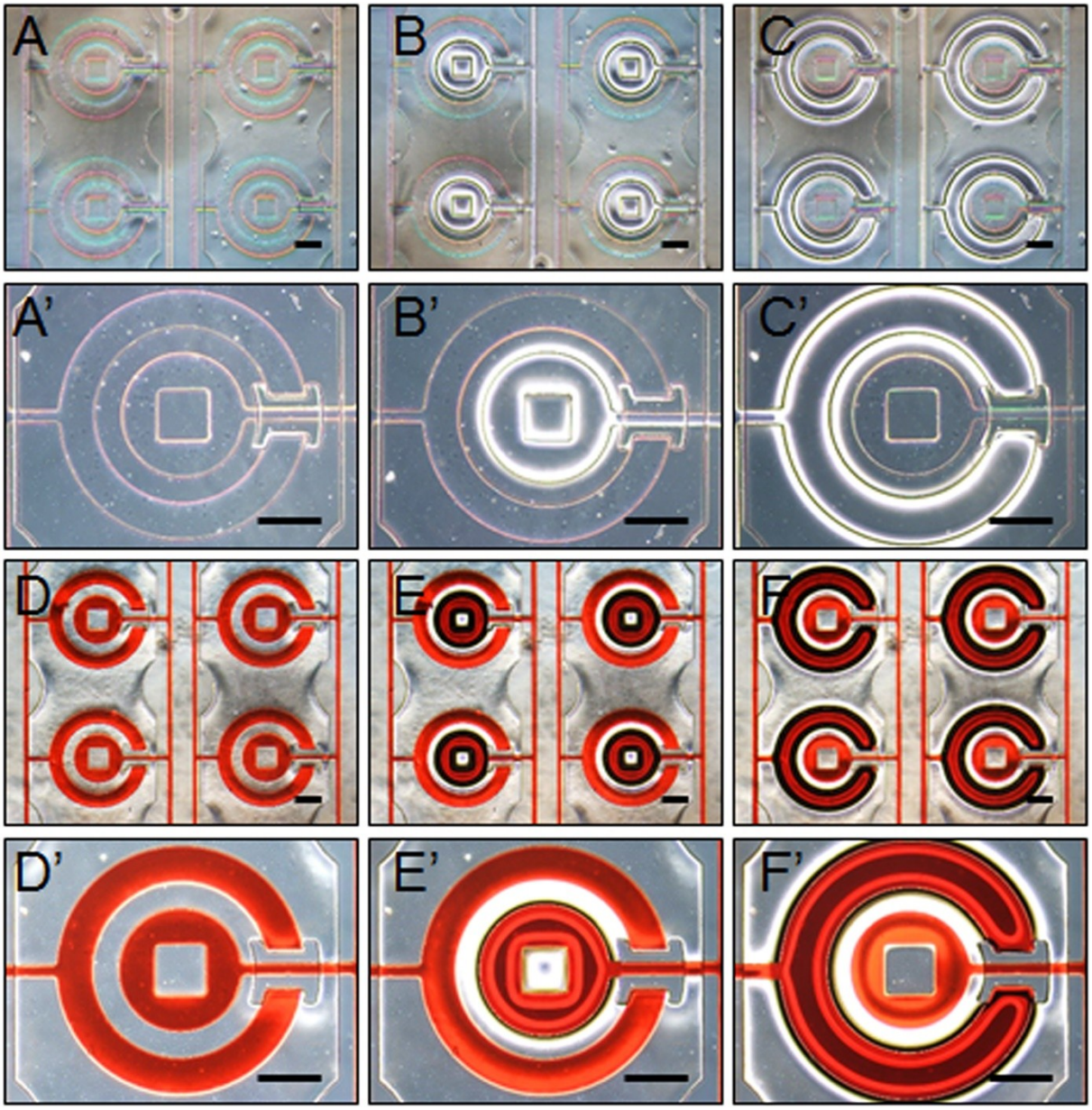

Figure S33. Display of the microfluidic device for generation of multi-compartmental cell-laden microgel with a square core hydrogel. (A) Bright-field image of the pneumatic microvalves in an array. (B) The actuation status of the inner ring-shape microvalves in an array. (C) The actuation status of the outer U-shape microvalves in an array. (A')-(C') The actuation status of a single microvalve, corresponding to (A)-(C). (D)-(F) and (D')-(F') The control channel of the microvalve was colored by being filled with red food dye, corresponding to (A)-(C) and (A')-(C'). Scale bar, 250 μm.

Supplementary Figure S34.

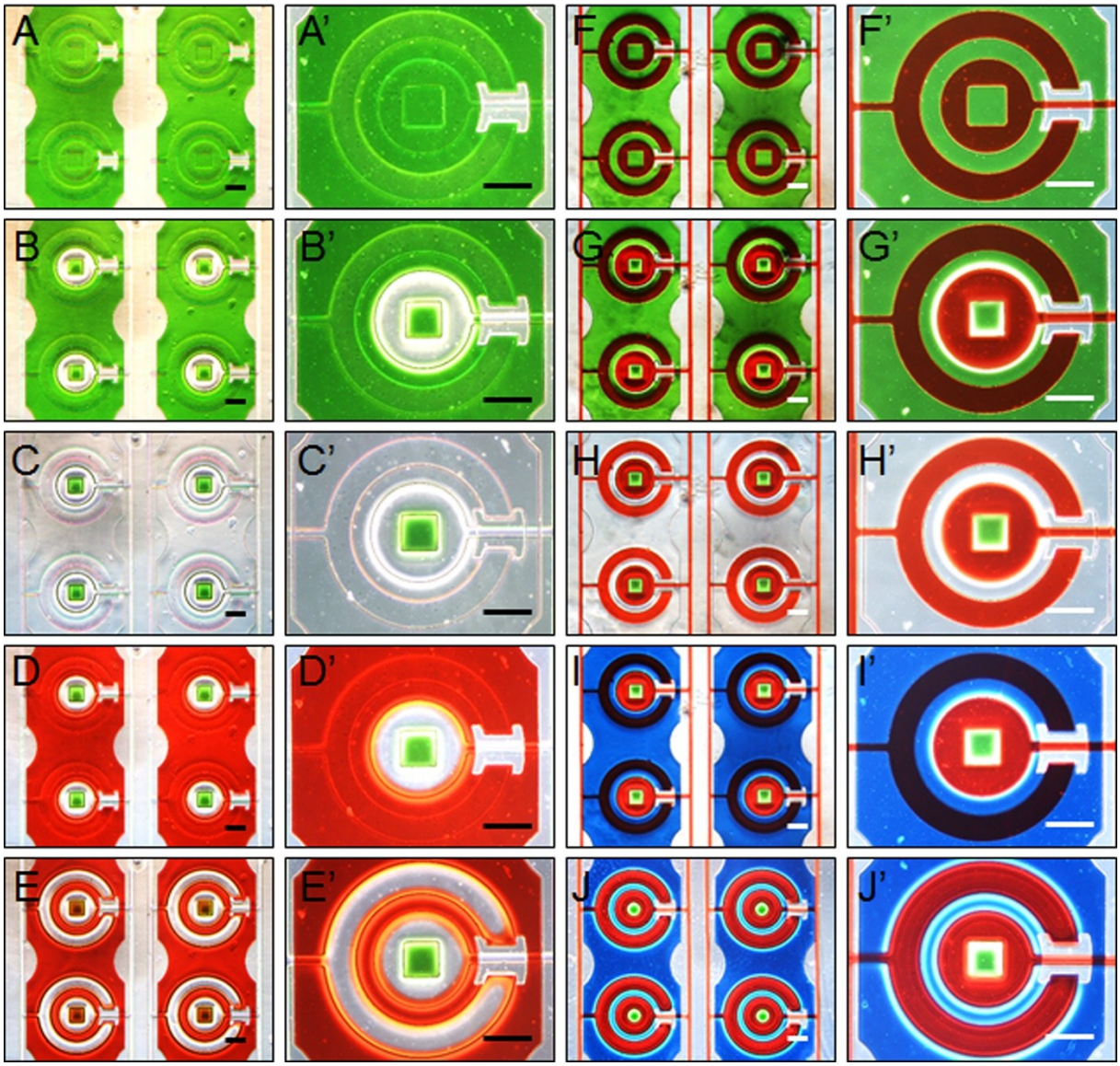

Figure S34. Display of the working flow of the microfluidic device for generation of multi-compartmental cell-laden microgel with a square core hydrogel. (A) The microfluidic device was filled with green food dye. (B) The inner ring-shape pneumatic microvalves were actuated to restrict the food dye in a first pattern. (C) A wash with water removed the unblocked food dye. (D) The microfluidic device was filled with red food dye. (E) The outer U-shape pneumatic microvalves were actuated to restrict the second food dye in a secondary pattern. (A')-(E') The actuation status of a single microvalve, corresponding to (A)-(E). (F)-(J) and (F')-(J') The control channel of the microvalve was colored by being filled with red food dye, corresponding to (A)-(E) and (A')-(E'). Scale bar, 250 μm.

Supplementary Figure S35.

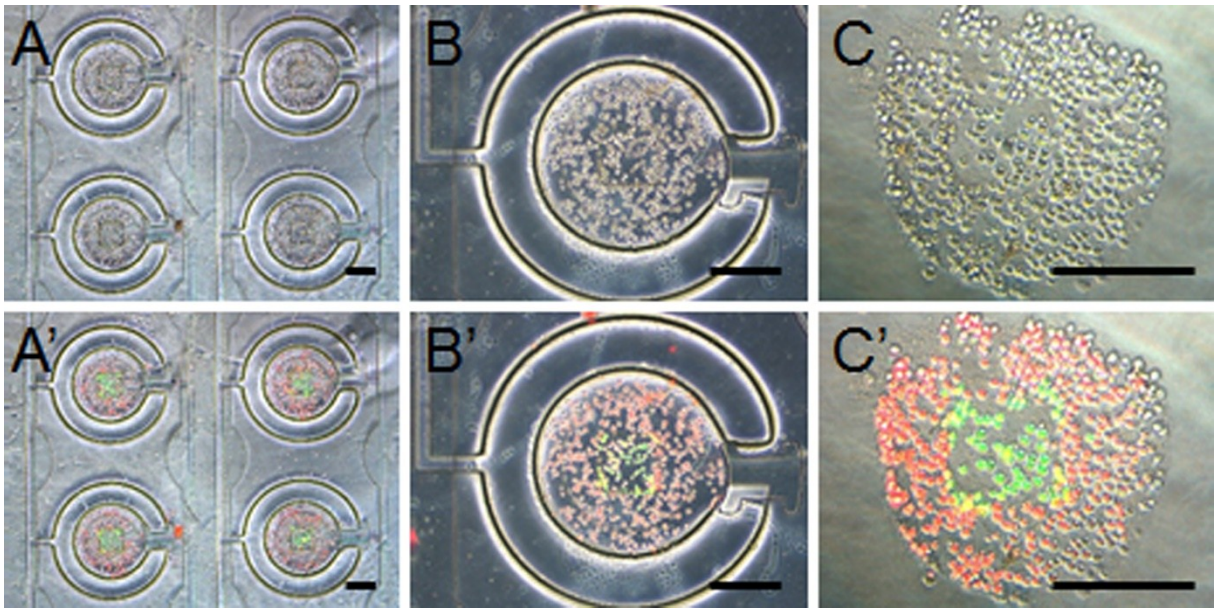

Figure S35. Generation of multi-compartmental cell-laden microgels with a square core hydrogel, corresponding to Figure 3C. (A) An on-chip array of cell-laden microgels. (B) A single microgel on-chip. (C) A single microgel harvested. (A')-(C') The merged images of bright-field images and fluorescent images, corresponding to (A)-(C). Scale bar, 250 μm.

Supplementary Figure S36.

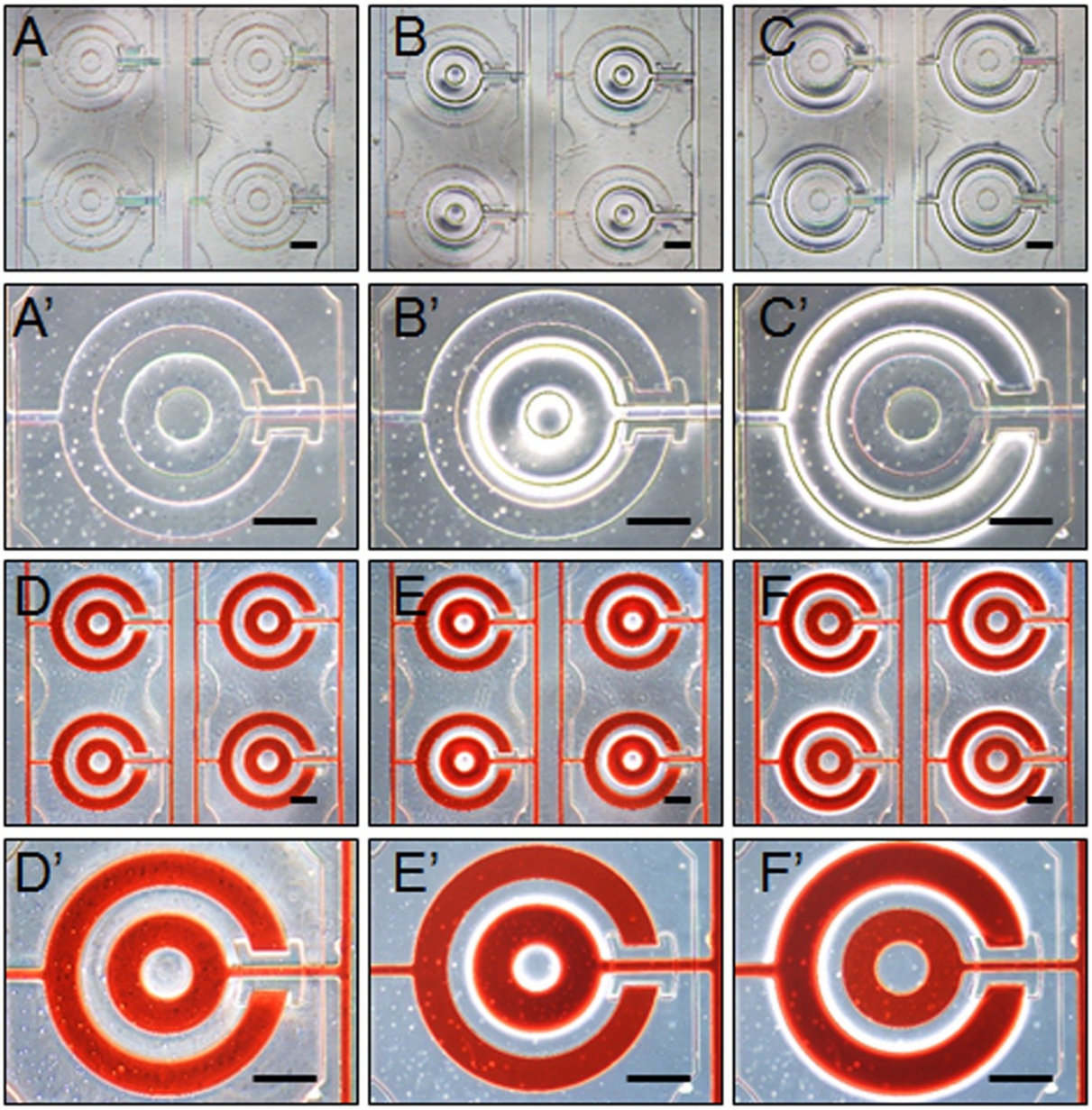

Figure S36. Display of the microfluidic device for generation of multi-compartmental cell-laden microgel with a circular core hydrogel. (A) Bright-field image of the pneumatic microvalves in an array. (B) The actuation status of the inner ring-shape microvalves in an array. (C) The actuation status of the outer U-shape microvalves in an array. (A')-(C') The actuation status of a single microvalve, corresponding to (A)-(C). (D)-(F) and (D')-(F') The control channel of the microvalve was colored by being filled with red food dye, corresponding to (A)-(C) and (A')-(C'). Scale bar, 250 μm.

Supplementary Figure S37.

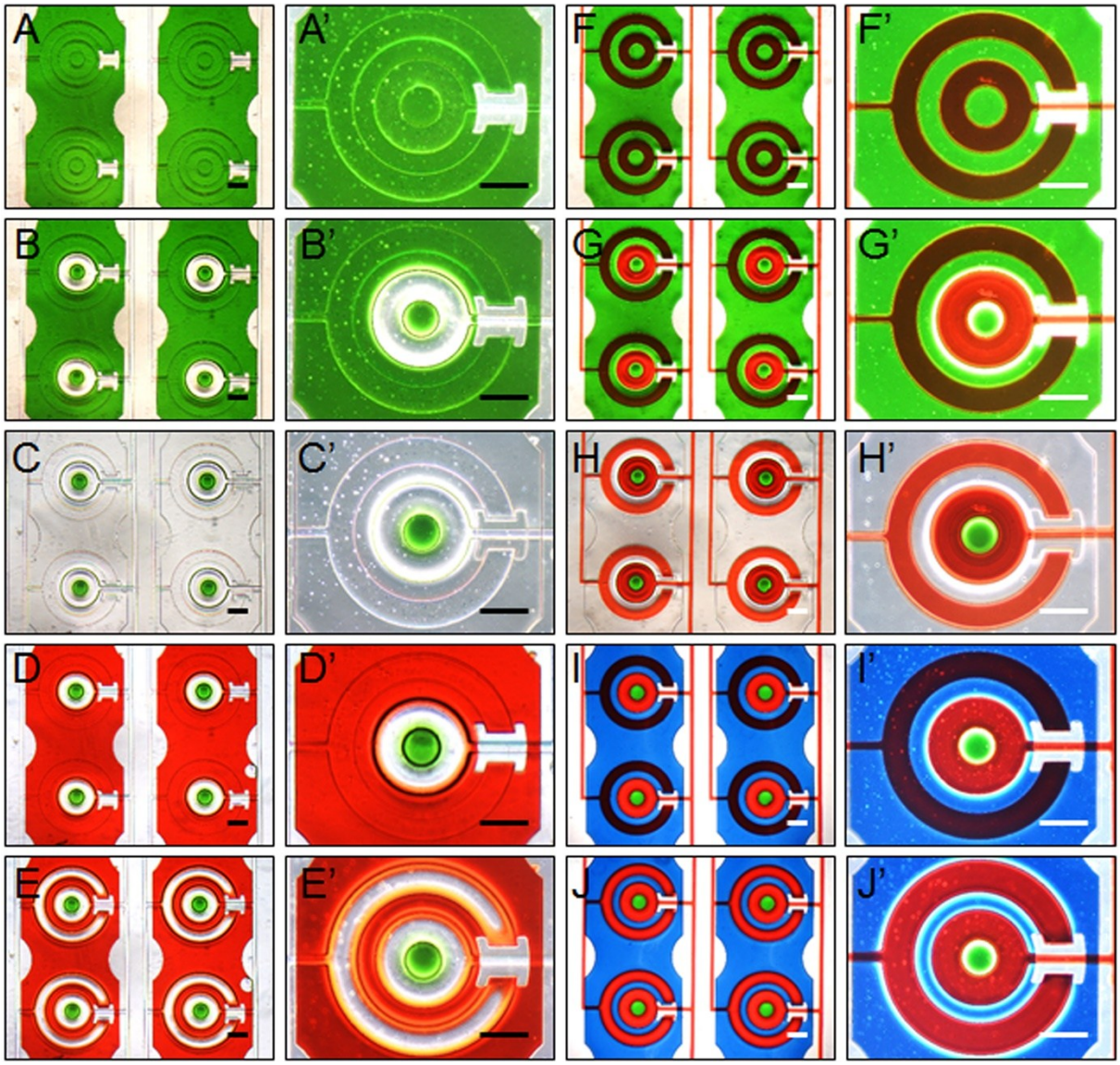

Figure S37. Display of the working flow of the microfluidic device for generation of multi-compartmental cell-laden microgel with a circular core hydrogel. (A) The microfluidic device was filled with green food dye. (B) The inner ring-shape pneumatic microvalves were actuated to restrict the food dye in a first pattern. (C) A wash with water removed the unblocked food dye. (D) The microfluidic device was filled with red food dye. (E) The outer U-shape pneumatic microvalves were actuated to restrict the second food dye in a secondary pattern. (A')-(E') The actuation status of a single microvalve, corresponding to (A)-(E). (F)-(J) and (F')-(J') The control channel of the microvalve was colored by being filled with red food dye, corresponding to (A)-(E) and (A')-(E'). Scale bar, 250 μm.

Supplementary Figure S38.

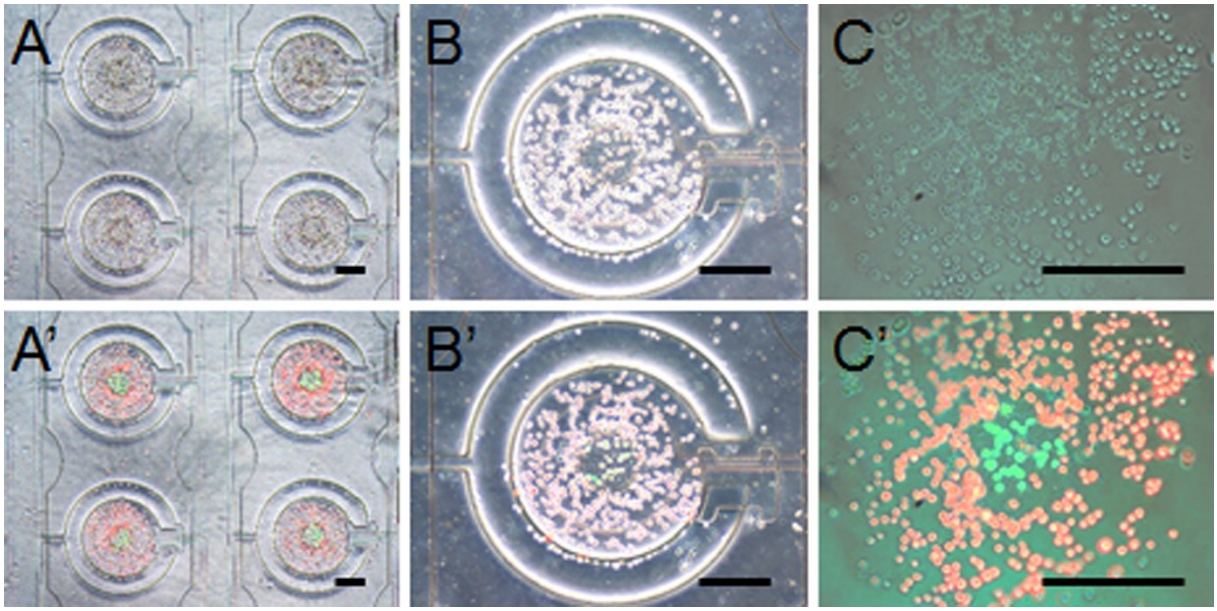

Figure S38. Generation of multi-compartmental cell-laden microgels with a circular core hydrogel, corresponding to Figure 3D. (A) An on-chip array of cell-laden microgels. (B) A single microgel on-chip. (C) A single microgel harvested. (A')-(C') The merged images of bright-field images and fluorescent images, corresponding to (A)-(C). Scale bar, 250 μm.

Supplementary Figure S39.

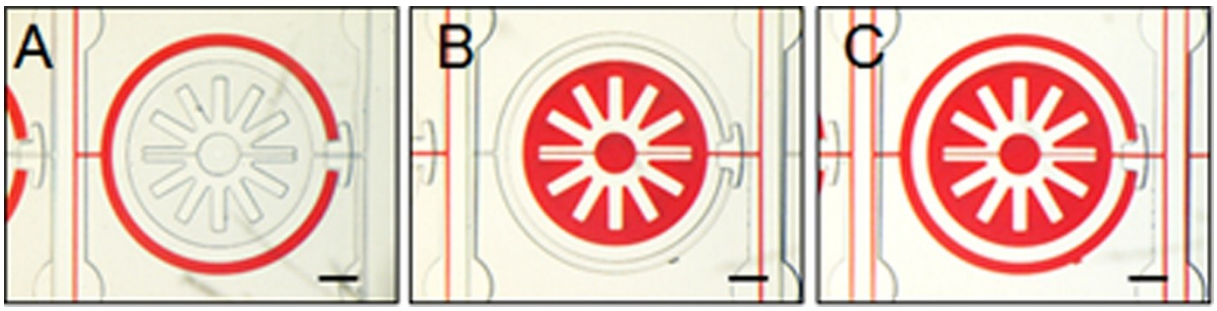

Figure S39. Display of the microfluidic device for generation of liver lobule-like cell-laden microgel. (A) The control channel of the inner microvalve was colored by being filled with red food dye. (B) The control channel of the outer microvalve was colored by being filled with red food dye. (C) The microvalve system was colored by being filled with red food dye. Scale bar, 500 μm.

Supplementary Figure S40.

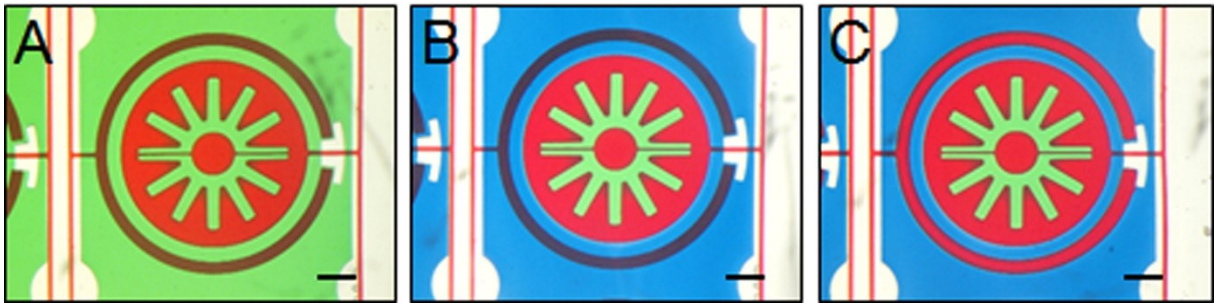

Figure S40. Display of the working flow of the microfluidic device for generation of liver lobule-like cell-laden microgel. The control channel of the microvalve was colored by being filled with red food dye. (A) The microfluidic device was filled with green food dye. The inner pneumatic microvalves were actuated to restrict the food dye in a first pattern. (B) After a wash with water to remove the unblocked food dye, the microfluidic device was filled with blue food dye. (C) The outer U-shape pneumatic microvalves were actuated to restrict the second food dye in a secondary pattern. Scale bar, 500 μm.

Supplementary Figure S41.

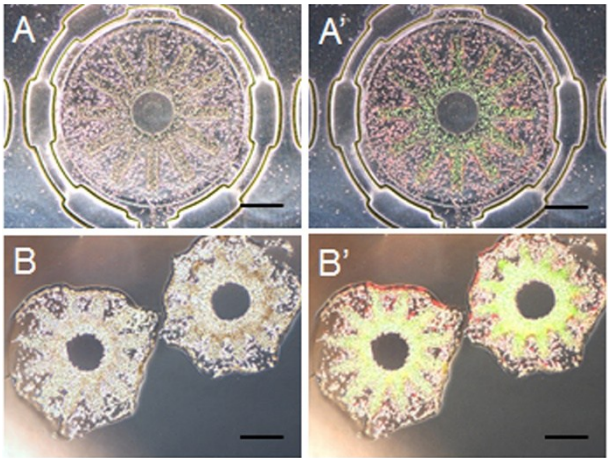

Figure S41. Generation of multi-compartmental cell-laden microgels with a liver lobule-like morphology, corresponding to Figure 4B. (A) An on-chip liver lobule-like microtissue. (B) The liver lobule-like microtissues harvested into cell culture media. (A') and (B') The merged images of bright-field images and fluorescent images. Scale bar, 500 μm.

Supplementary Figure S42.

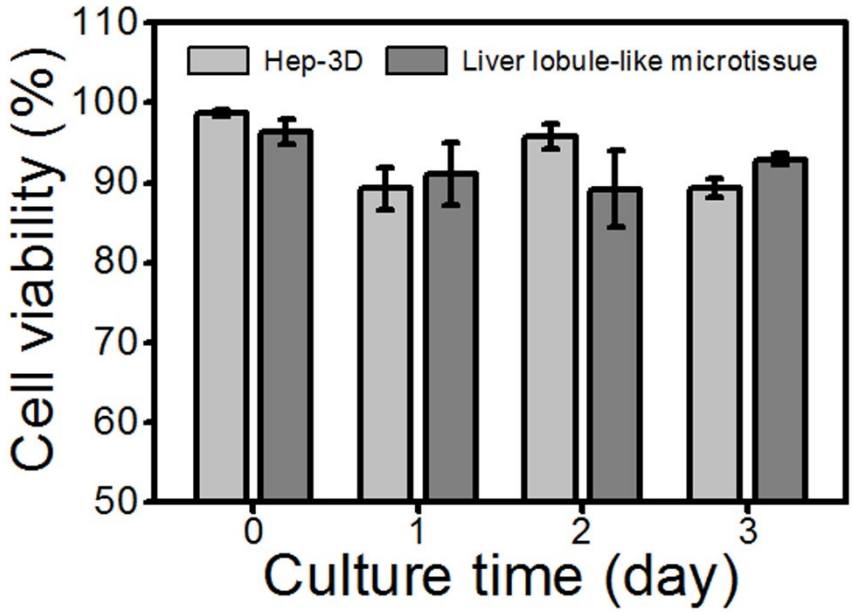

Figure S42. Quantitative data of the viability of HepG2 cells in the liver lobule-like microtissue during a 3-day culture, with 3D monocultured HepG2 cells (i.e., Hep-3D) as a control. Data are given as means ± SD, and collected from three independent experiments. The result showed that the hepatocytic viability was greater than 90% after encapsulation into the hydrogel matrix and along the 3-day culture, suggesting that the cell loading process did not cause observable mechanical damage to the cells, and the liver models could be used for the following study.